frontiers | Frontiers in Astronomy and Space Sciences

TYPE Review
PUBLISHED 15 March 2024
DOI 10.3389/fspas.2024.1356379

OPEN ACCESS

EDITED BY
Christoffer Karoff,
Aarhus University, Denmark

REVIEWED BY
Javier Pascual Granado,
Spanish National Research Council (CSIC), Spain
Martin Nielsen,
University of Birmingham, United Kingdom

*CORRESPONDENCE
Ângela R. G. Santos,
✉ Angela.Santos@astro.up.pt

RECEIVED 15 December 2023
ACCEPTED 19 February 2024
PUBLISHED 15 March 2024

CITATION
Santos ÂRG, Godoy-Rivera D, Finley AJ, Mathur S, García RA, Breton SN and Broomhall A-M (2024), *Kepler* main-sequence solar-like stars: surface rotation and magnetic-activity evolution.
Front. Astron. Space Sci. 11:1356379.
doi: 10.3389/fspas.2024.1356379

Kepler main-sequence solar-like stars: surface rotation and magnetic-activity evolution

Ângela R. G. Santos[1]*, Diego Godoy-Rivera[2,3], Adam J. Finley[4], Savita Mathur[2,3], Rafael A. García[4], Sylvain N. Breton[5] and Anne-Marie Broomhall[6]

[1]Instituto de Astrofísica e Ciências do Espaço, Universidade do Porto, CAUP, Porto, Portugal, [2]Instituto de Astrofísica de Canarias (IAC), Tenerife, Spain, [3]Universidad de La Laguna (ULL), Departamento de Astrofísica, Tenerife, Spain, [4]Université Paris-Saclay, Université Paris Cité, CEA, CNRS, AIM, Gif-sur-Yvette, France, [5]INAF–Osservatorio Astrofisico di Catania, Catania, Italy, [6]Department of Physics, University of Warwick, Coventry, United Kingdom

While the mission's primary goal was focused on exoplanet detection and characterization, *Kepler* made and continues to make extraordinary advances in stellar physics. Stellar rotation and magnetic activity are no exceptions. *Kepler* allowed for these properties to be determined for tens of thousands of stars from the main sequence up to the red giant branch. From photometry, this can be achieved by investigating the brightness fluctuations due to active regions, which cause surface inhomogeneities, or through asteroseismology as oscillation modes are sensitive to rotation and magnetic fields. This review summarizes the rotation and magnetic activity properties of the single main-sequence solar-like stars within the *Kepler* field. We contextualize the *Kepler* sample by comparing it to known transitions in the stellar rotation and magnetic-activity evolution, such as the convergence to the rotation sequence (from the saturated to the unsaturated regime of magnetic activity) and the Vaughan-Preston gap. While reviewing the publicly available data, we also uncover one interesting finding related to the intermediate-rotation gap seen in *Kepler* and other surveys. We find evidence for this rotation gap in previous ground-based data for the X-ray luminosity. Understanding the complex evolution and interplay between rotation and magnetic activity in solar-like stars is crucial, as it sheds light on fundamental processes governing stellar evolution, including the evolution of our own Sun.

KEYWORDS

stars: activity, stars: evolution, stars: late-type, stars: low-mass, stars: magnetic field, stars: rotation, stars: solar-type, starspots

1 Introduction

Low-mass stars with convective outer layers, also known as solar-like stars, can sustain internal dynamos and have the potential to harbor magnetic activity. Magnetic fields and magnetic cycles are generated by an interaction between differential rotation and convection (see Brun and Browning, 2017, for a recent review). As the strong magnetic fields emerge at the stellar photosphere, they form active regions, where dark spots appear, usually in pairs or groups of opposite polarity (e.g., Hale et al., 1919; Solanki, 2003; Hathaway, 2015). Such active regions can be associated with eruptive events like flares and coronal mass ejections (e.g., Zirin, 1970; Solanki, 2003). As active regions decay their magnetic fields disperse and

concentrate at the edges of the convective cells, forming the bright faculae (e.g., van Driel-Gesztelyi and Green, 2015). In the chromosphere, these regions of intermediate magnetic-field strength appear as bright plage. All these phenomena are part of the star's magnetic activity, which varies at different timescales. In particular, the Sun undergoes an 11-year cycle of magnetic activity. Analogously, other stars are known to exhibit magnetic activity cycles (e.g., Baliunas et al., 1995; Oláh et al., 2009; García et al., 2010; Boro Saikia et al., 2018; Karoff et al., 2018), with cycle periods ranging from a few years to over 20 years. As the dynamo mechanism is powered by the interplay of convection and rotation (e.g., Brun and Browning, 2017), the cycle and rotation periods are found to be related, with slow-rotating stars having longer cycles than fast-rotating stars. Stars are often seen to group along two branches: active and inactive (e.g., Brandenburg et al., 1998; Böhm-Vitense, 2007). However, there is still debate whether these are properly determined or even exist (e.g., Boro Saikia et al., 2018; Bonanno and Corsaro, 2022).

The level of magnetic activity is also intrinsically linked to rotation (e.g., Kraft, 1967; Pallavicini et al., 1981; Walter and Bowyer, 1981; Noyes et al., 1984; Soderblom et al., 1993; Pizzolato et al., 2003). At the beginning of their main-sequence lifetime, stars are relatively fast rotators and exhibit high activity levels (e.g., Skumanich, 1972; Barnes, 2003b; Fritzewski et al., 2021a; Brown et al., 2021). Stars gradually lose angular momentum due to their magnetized winds (e.g., Kraft, 1967; Weber and Davis, 1967; Skumanich, 1972; Kawaler, 1988; Pinsonneault et al., 1989; Gallet and Bouvier, 2013; Matt et al., 2015), in a process known as magnetic braking. The rate at which the stars spin down depends on their rotation, with faster rotators losing angular momentum faster than slower rotators. Eventually, stars will converge into the so-called slow-rotation sequence (see for example, Figure 3 in Gallet and Bouvier, 2013), and from that point onwards the rotation rate decays proportionally to the square root of the age, known as the Skumanich spin-down law (Skumanich, 1972). The spin-down process is also mass-dependent, with lower-mass stars taking longer to converge into the rotation sequence than higher-mass stars, but once reached, lower-mass stars spin down faster than higher-mass stars (e.g., Barnes, 2003b; Barnes, 2007; van Saders and Pinsonneault, 2013; Matt et al., 2015). The magnetic activity also decays with time: as stars evolve and spin down, they gradually become less active (Wilson, 1963; Skumanich, 1972; Soderblom et al., 1991). Therefore, generally, fast-rotating stars have stronger magnetic activity than slow-rotating stars. This activity-rotation relationship can be represented as a function of the Rossby number, Ro (Noyes et al., 1984). Ro can be defined as the ratio between the star's rotation period and its convective turnover timescale. The latter corresponds to the typical timescale for convective motions in the stars' envelopes and remains mostly constant during the main-sequence lifetime, increasing as the effective temperature decreases (e.g., Lehtinen et al., 2021). Metallicity, however, can complicate this picture. Due to a larger opacity, metal-rich stars have deeper convection zones than their metal-poor counterparts (e.g., van Saders and Pinsonneault, 2012). A deeper convection zone leads to a more vigorous dynamo, consequently to higher magnetic activity. Observational evidence for this effect has been found in both large samples (See et al., 2021; See et al., 2023) and in the particular case of the seismic solar-analog HD 173701 (KIC 8006161). This ~1$M_{\odot}$ star exhibits a magnetic cycle with more than twice the amplitude of the solar cycle (Karoff et al., 2018). Strong magnetic activity, in turn, would lead to a more efficient loss of the angular momentum. Thus, metal-rich stars are expected to spin down faster than metal-poor stars (Amard and Matt, 2020) and, so far, this theoretical expectation has been supported by observations (e.g., Amard et al., 2020; Santos et al., 2023).

The Skumanich spin-down law led to the development of gyrochronology (e.g., Barnes, 2003b; Barnes, 2007; Mamajek and Hillenbrand, 2008; García et al., 2014a; Angus et al., 2015; Lu et al., 2023), enabling estimation of stellar ages from surface rotation. Analogously, magnetochronology and magnetogyrochronology relations have also been established (e.g., Mamajek and Hillenbrand, 2008; Pace, 2013; Lorenzo-Oliveira et al., 2018; Mathur et al., 2023; Ponte et al., 2023). As rotation and magnetic activity measurements are available for large numbers of stars, these techniques are powerful tools for estimating stellar ages. However, the evolution of stellar rotation and magnetic activity is not yet fully understood, as we will discuss below.

The stars' magnetic fields can be measured through Zeeman Broadening of spectral lines and Zeeman Doppler Imaging (ZDI; e.g., Semel, 1989; Donati and Brown, 1997; Reiners et al., 2022; Vidotto et al., 2014; See et al., 2019a; Brown et al., 2022, see also Kochukhov, 2021 for a recent review). These techniques shed light on the evolution of stellar magnetic fields and allow the large-scale magnetic field topology to be recovered. The ZDI technique has been used to follow entire stellar magnetic cycles which, in the case of 61 Cyg A, share many similarities to that of the solar cycle (Saikia et al., 2018). However, due to the challenges of directly measuring magnetic fields, indirect measures are often used. These are magnetic activity proxies and link to phenomena associated with the presence of strong magnetic fields, which can be constrained by spectroscopic and photometric observations.

In spectroscopy, magnetic activity is often constrained through the analysis of particular spectral lines. Examples of such lines are the Ca II H & K lines in the near ultra-violet (NUV) and the Ca II infrared triplet (IRT). In the presence of active regions, these absorption lines show emission at their cores due to chromospheric heating. By measuring such emission and removing the basal and photospheric contributions, these lines provide proxies for magnetic activity in the chromosphere (e.g., Leighton, 1959; Wilson, 1968; Wilson, 1978; Baliunas et al., 1995; Karoff et al., 2016; Fritzewski et al., 2021a; Gomes da Silva et al., 2021). Since active regions go in and out of view as the star rotates, these activity proxies can show short-term quasi-periodic variations, allowing to constrain rotation periods (e.g., Suárez Mascareño et al., 2017; Lorenzo-Oliveira et al., 2019). Another activity proxy that can be derived from spectra is the spot filling factor (e.g., Gully-Santiago et al., 2017; Cao and Pinsonneault, 2022; Gosnell et al., 2022), which follows upon the fact that magnetic spots in solar-like stars are cool features in comparison to their surroundings.

In white-light photometry, active regions lead to variations in the stellar brightness, known as rotation modulation. Once again, as active regions co-rotate, in this case with the stellar surface, the periodicity of these brightness variations is related to the surface rotation period at the latitudes where the active regions are formed (e.g., Gaidos et al., 2000; Reinhold et al., 2013; García et al., 2014a; McQuillan et al., 2014; Lanzafame et al., 2018;

Gordon et al., 2021; Santos et al., 2021; Lu et al., 2022; Claytor et al., 2023; Distefano et al., 2023). The amplitude of the brightness variations relates to the surface coverage by active regions (e.g., Basri et al., 2010; García et al., 2010; Mathur et al., 2014b; Salabert et al., 2017) and is found to be well correlated with chromospheric activity proxies (Salabert et al., 2016; Ponte et al., 2023). One of the advantages associated with the advent of photometric space missions is that they allow the retrieval of magnetic activity proxies and rotation for stellar samples orders of magnitude larger than those from ground-based surveys.

Stellar flares can also be detected and characterized from white-light photometry (e.g., Davenport, 2016; Ilin et al., 2019; Ilin et al., 2021; Yang and Liu, 2019; Günther et al., 2020), providing a proxy for magnetic activity. Another widely used magnetic activity proxy is X-ray emission from hot plasma confined in coronal loops (e.g., Schmitt et al., 1995; Pizzolato et al., 2003; Pillitteri et al., 2006; Wright et al., 2018), which is correlated with the stellar wind mass-loss rates (Wood et al., 2021). Other activity indicators used in the literature are the Hα emission and NUV excess (e.g., Findeisen et al., 2011; Newton et al., 2017; Godoy-Rivera et al., 2021b; Zhong et al., 2023).

Asteroseismology can also be effective in measuring rotation and magnetic activity in solar-like stars, thanks to the acoustic modes (p modes) being sensitive to both properties. In this case, solar-like acoustic oscillations give information mostly from subphotosphere layers (e.g., Basu et al., 2012; Benomar et al., 2015). Rotation can be measured from the splitting of the modes' azimuthal orders if the stellar inclination angle is not too small (Gizon and Solanki, 2003; Ballot et al., 2006, inclination of 90° and 0° correspond, respectively, to observing the star equator-on and pole-on). In addition to an average rotation (e.g., Gizon et al., 2013; Davies et al., 2015; Hall et al., 2021), asteroseismology also allows us to obtain information about surface latitudinal differential rotation (Benomar et al., 2018; Bazot et al., 2019). Unfortunately, main-sequence solar-like stars pose a significant challenge in the determination of their radial differential rotation due to uncertainties in observations and stellar models (Benomar et al., 2015; Schunker et al., 2016b; Schunker et al., 2016a; Nielsen et al., 2017). Moreover, the number of visible modes is limited, as well as their sensitivity to greater depths in the stellar interiors. Magnetic activity affects different properties of the acoustic modes (e.g., Woodard and Noyes, 1985; Elsworth et al., 1990; Jiménez-Reyes et al., 1998; Jain et al., 2009; García et al., 2010; Tripathy et al., 2011; Broomhall et al., 2014; Kiefer et al., 2017; Santos et al., 2018). Particularly, the mode frequencies are observed to increase with the magnetic activity level, while mode amplitudes decrease. For low-degree modes, those that are possible to observe for stars other than the Sun, modes of different angular degrees are affected differently by stellar activity (e.g., Jiménez-Reyes et al., 1998; Chaplin et al., 2004; Broomhall et al., 2012; Salabert et al., 2015), depending on the latitudes where active regions emerge (active latitudes). This fact reveals another capability of asteroseismology, in this case, to constrain active latitudes in stars by investigating the magnetic signatures in modes of different angular degrees, as it was done for the well-characterized solar-analog HD 173701 by Thomas et al. (2019). However, the suppression of mode amplitudes by magnetic activity prevents the detection of acoustic modes in stars with strong magnetic activity (Chaplin et al., 2011; Mathur et al., 2019; Gehan et al., 2022; Gehan et al., 2024). Therefore, seismic samples are biased towards weakly active slow rotators.

The *Kepler* mission (Borucki et al., 2010), launched by NASA (National Aeronautics and Space Administration), provided one of the most significant contributions to the expansion of stars with known surface rotation and measured activity levels (e.g., McQuillan et al., 2013; McQuillan et al., 2014; Nielsen et al., 2013; Reinhold et al., 2013; Reinhold et al., 2023; García et al., 2014a; Ceillier et al., 2017; Santos et al., 2019; Santos et al., 2021). Comparatively, *Gaia*, launched by ESA (European Space Agency), has yielded a much larger number of rotation measurements (Lanzafame et al., 2018; Distefano et al., 2023). Nevertheless, *Kepler* and *Gaia* yields are complementary (e.g., Lanzafame et al., 2019), with *Kepler* probing typically slower rotators than *Gaia*, including stars similar to our Sun (for reference, at 5,000 K, the 5th and 95th percentiles of *Kepler* $P_{\rm rot}$ distribution are 8.2 and 38.8 days, while the analogous limits for *Gaia* are 0.4 and 12.6 days). *Kepler* revealed two potential deviations to the Skumanich spin-down law, whose origins are still under debate.

Most of the *Kepler* main-sequence sample has already converged to the slow-rotation sequence, where the Skumanich spin-down law is generally assumed to be valid. However, *Kepler* data suggests the existence of a transition within this regime, with the surface rotation distribution being bimodal (e.g., McQuillan et al., 2013; McQuillan et al., 2014; Davenport and Covey, 2018; Santos et al., 2019; Santos et al., 2021), which is particularly evident at low temperatures, resulting on an intermediate-rotation gap (~15 days at 4500 K). Spin-down stalling, likely associated with this gap, is evident in stellar clusters with ages around 1 Gyr (Curtis et al., 2019). Recently the intermediate-rotation gap was found in K2 (Howell et al., 2014) and ground-based data for partially convective stars (Reinhold and Hekker, 2020; Gordon et al., 2021; Lu et al., 2022), but is absent in fully convective stars (Lu et al., 2022). Different hypotheses to explain the gap were proposed, with the core-envelope coupling theory gaining traction (e.g., McQuillan et al., 2014; Angus et al., 2020; Spada and Lanzafame, 2020; Gordon et al., 2021; Lu et al., 2022). In this scenario, the angular momentum transfer between the stars' fast core and slow envelope would momentarily stall the spin-down. Once the coupling is completed, the Skumanich-like spin-down would resume.

The second transition *Kepler* unveiled concerns relatively old main-sequence stars, around the age of the Sun and older. Given their asteroseismic ages, some of these stars spin faster than expected if their spin-down was consistent with the Skumanich law (Angus et al., 2015; van Saders et al., 2016; Hall et al., 2021). This observation led to the formulation of the weakened magnetic braking (WMB), which would take place around the middle of the main-sequence lifetime, at a given critical Ro (e.g., Metcalfe et al., 2016; van Saders et al., 2016; Metcalfe and van Saders, 2017; Saunders et al., 2023). Despite the observational support for WMB, its physical cause(s) remains unclear. As the efficiency of angular momentum transport is primarily governed by the stellar magnetic field (Réville et al., 2015), one possible explanation is that the stellar dynamo becomes less efficient, leading to a weaker or more complex magnetic field configuration (explored in numerical experiments,

e.g., Brun et al., 2022). This hypothesis has been investigated using spectropolarimetric observations of solar-like stars, which recover the large-scale magnetic field strength and topology (See et al., 2019b; Metcalfe et al., 2021; Metcalfe et al., 2022). Other explanations range from the influence of latitudinal differential rotation (Tokuno et al., 2023), to decreases in the stellar wind mass-loss rates due to closed magnetic fields (Garraffo et al., 2016) or less efficient wind heating/acceleration (Shoda et al., 2020). As the Sun lies around this transition, attempts have been made to measure the present-day solar wind braking torque (Finley et al., 2019b). Both observations and numerical models show the braking torque to be a factor of two to three times smaller than required by the Skumanich relation (Matt et al., 2015; Finley et al., 2018), lending support to the weakened braking hypothesis.

Looking to the magnetic-activity evolution, another transition may exist, the so-called Vaughan-Preston (VP) gap (e.g., Vaughan, 1980; Vaughan and Preston, 1980; Henry et al., 1996; Gomes da Silva et al., 2021). The VP gap is characterized by a lack of stars with intermediate Ca II H & K emission. However, there is extensive debate in the community surrounding its existence. In particular, when exploring larger and more complete samples, the VP gap attenuates and in some cases almost disappears (e.g., Boro Saikia et al., 2018; Brown et al., 2022). Although Brown et al. (2022) did not find a clear gap, the authors also found evidence supporting a phase of rapid evolution, consistent with the parameter space of the VP gap. Therefore, it is not clear yet whether the VP gap is a result of a transition in the magnetic-activity evolution or a result of observational bias. So far, there is no evidence for it in *Kepler* data.

These recent discrepancies between the observations and the expected behavior reinforce the need for a better understanding of rotation and magnetic-activity evolution. This review places the *Kepler* rotational sample in the context of the known transitions during the main sequence and describes them in more detail in the following sections.

2 *Kepler* main-sequence solar-like rotation sample

The *Kepler* mission provided exquisite data for stellar physics. In addition to high-precision photometry, *Kepler* monitored the same stars in a continuous, long-term manner, spanning up to 4 years of observations. Still, *Kepler* data are not free of systematics and instrumental artifacts. Therefore, it is important to correct and calibrate them (e.g., Jenkins et al., 2010; García et al., 2011; 2014b), while preserving stellar signals at long timescales, such as the rotation modulation of slow rotators. Once processed, *Kepler* data constrained surface rotation periods and photometric magnetic activity for several tens of thousands of solar-like stars from the main-sequence to the red-giant phase (e.g., García et al., 2014a; McQuillan et al., 2014; Ceillier et al., 2017; Santos et al., 2019; 2021). While the focus of this review is the main-sequence (MS) solar-like stars, it is worth noting that magnetic fields and activity are also found in earlier spectral types (e.g., Balona, 2015; Balona, 2019; Mathys, 2017; Henriksen et al., 2023).

We begin with the sample of 55,252 stars with known rotation periods from Santos et al. (2019), Santos et al. (2021)[1], which included subgiant stars by design. To select solely the MS stars we adopt the selection criteria based on the color-magnitude diagram (CMD) from *Gaia* Data Release 3 (Gaia Collaboration et al., 2023), as detailed in Appendix A of García et al. (2023). The magnitudes were corrected for extinction and the selection criteria also remove potential binaries and outliers that sit above or below the MS in the CMD, as well as targets with large (≥1.2) renormalized united weighted error (RUWE; Gaia Collaboration et al., 2023), *Gaia* radial velocity variables (Katz et al., 2023), stars in the *Gaia* non-single-star sample (Gaia Collaboration et al., 2023), and eclipsing binaries (Kirk et al., 2016). As we do not yet fully understand the rotational signals from targets flagged as close-in binary candidates in Santos et al., 2019; Santos et al., 2021, we keep those that pass the criteria (1,311 targets). This leaves us with a reference *Kepler* sample of 34,898 single MS stars with known rotation rates. The selection criteria are relatively stringent to ensure a clean sample. Applying the same criteria to the sample of McQuillan et al. (2014) would reduce it to 21,685 stars. Comparing the respective clean samples, we verify that the latest catalog still pushed the upper edge of the rotation-period distribution towards slower rotators (see Figure 12 in Santos et al., 2021).

The top panel of Figure 1 shows the *Kepler* rotation MS sample. The dashed lines mark the upper and lower edges of the $P_{\rm rot}$ distribution, corresponding to the 95th and 5$^{\rm th}$ percentiles, whose origin is discussed in more detail below. In general, hotter stars are fast rotators than cooler stars, which is expected, as for most of the MS, the magnetic braking is more efficient for less massive stars (van Saders and Pinsonneault, 2013; Matt et al., 2015). Another feature that can be seen in the *Kepler* sample is the so-called intermediate-$P_{\rm rot}$ gap, leading to a bimodal $P_{\rm rot}$ distribution. For cooler solar-like stars (K and M), a lower-density region, in between two populations or sequences of stars, can be found. For G dwarfs, the lower density region disappears but the $P_{\rm rot}$ distribution is still bimodal (e.g., Davenport, 2017). The dot-dashed line indicates the intermediate-$P_{\rm rot}$ gap computed for the clean sample as described in Santos et al. (2023).

For the *Kepler* sample, the magnetic activity is quantified from the rotational modulation in the light curve using the activity proxy $S_{\rm ph}$, computed in Santos et al. (2019), Santos et al. (2021) as defined by Mathur et al. (2014a), Mathur et al. (2014b), see also García et al. (2010). The bottom panels of Figure 1 show the activity-rotation diagram for the *Kepler* MS sample split by spectral type ($T_{\rm eff}$ boundaries at 3700, 5200, and 6000 K). Generally, fast rotators are more magnetically active than slow rotators. The black solid lines show the respective density contours, as reference for the figures below. GKM stars are color-coded according to their location concerning the intermediate-$P_{\rm rot}$ gap. The color code for the F stars indicates whether their $T_{\rm eff}$ is below or above the Kraft break (6250 K; Kraft, 1967). While the activity and rotation of cool F stars are correlated, similarly to the case of the GKM stars, hot F stars tend to

1 KEPSEISMIC light curves were adopted in these works and are available on MAST (Mikulski Archive for Space Telescopes): DOI: 10.17909/t9-mrpw-gc07; https://archive.stsci.edu/prepds/kepseismic/.

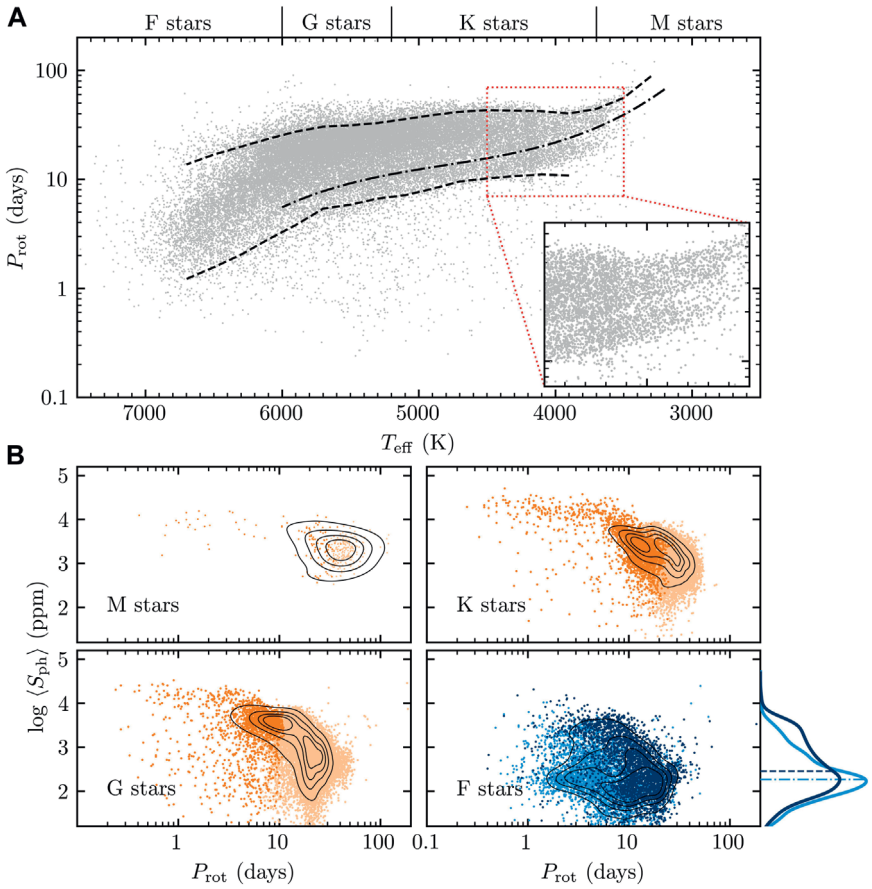

FIGURE 1
Summary figure of the sample of *Kepler* MS solar-like stars with known P_{rot}, illustrating the parameter space probed by *Kepler*. **(A)**: P_{rot} as a function of T_{eff}. The dashed black lines mark the upper and lower edges of the P_{rot} distribution. The black dot-dashed line marks the intermediate-P_{rot} gap. The subpanel shows a zoom-in into the low-temperature regime. To better see the intermediate-P_{rot} gap, we removed the lines. **(B)**: Activity-rotation diagrams for each spectral type. The solid lines mark the density contours. Orange and beige symbols correspond to stars faster and slower than the intermediate-P_{rot} gap, respectively. Dark and light blue show F stars cooler and hotter than the Kraft break, respectively. The side panel shows the corresponding S_{ph} distributions and median values.

be fast rotators with low activity levels (see also Appendix B in Santos et al., 2021). The solid blue lines show the S_{ph} distribution for F stars cooler and hotter than the Kraft break, whose median values are indicated by the dashed and dot-dashed lines (287.8 ppm and 185.8 ppm, respectively). This behavior can be explained by the shallow convective envelopes of the latter, which are unable to produce a strong magnetic field yielding inefficient magnetic braking (e.g., van Saders and Pinsonneault, 2013).

Below we discuss the transitions and detection biases in the *Kepler* rotation sample. We discuss other transitions that happen in a regime not probed by *Kepler* or, if probed, are not observed in *Kepler* data. In the activity-rotation figures, we opt to show P_{rot} and not Ro, as P_{rot} can be measured directly from the observations. In addition, the comparison between Ro numbers from different studies is not straightforward, as Ro depends on the adopted definition for the convective turnover timescale. Nevertheless, to split the samples into different regimes, when possible, we adopt the Ro number and the respective transitions as determined by the authors in the respective original studies.

3 From saturated to unsaturated: convergence to the rotation sequence

The members of young open clusters exhibit a wide range of rotation periods (e.g., Stauffer and Hartmann, 1987; Soderblom et al., 1993; Barnes, 2003b), consistent with stars transitioning from an ultra-fast rotation (a result of spin-up due to contraction onto the main sequence) to the converged rotation sequence. These two regimes are separated by a lower-density region, i.e., a gap at ultra-fast rotation (few days, depending on T_{eff}; Barnes, 2003b). The signature of this transition can also be identified in the magnetic activity of low-mass stars, particularly in their X-ray emission (Wright et al., 2011). Two regimes in the coronal magnetic activity are found by Wright et al. (2011): a *saturated* regime where X-ray emission is almost independent on P_{rot}; and a *unsaturated* regime where X-ray emission strongly depends on rotation, corresponding to the converged rotation sequence. The ultra-fast-P_{rot} bimodality found by Barnes (2003b) marks the transition from saturated to unsaturated magnetic activity. [Barnes (2003a), Barnes (2003b), hereafter B2003] proposed that

this transition is related to the core-envelope coupling, where the core and envelope would be coupled for stars in the converged rotation sequence (B2003's *interface* sequence), and decoupled for ultra-fast rotators (B2003's *convective* sequence). However, fully convective M dwarfs also follow the same activity-rotation relation characterized by the saturated and unsaturated regimes (Wright and Drake, 2016; Wright et al., 2018). Alternatively, Brown (2014) attributed the rotation gap to a transition between weak (saturated) to strong (unsaturated) coupling with the stellar wind, which in turn might be related to a transition from complex to simple magnetic field morphology (Réville et al., 2015; Garraffo et al., 2018).

Physically motivated models of angular momentum evolution can describe the observed convergence of rotation, particularly reproducing the mass-dependence of the spin-down (e.g., van Saders and Pinsonneault, 2013; Matt et al., 2015). Lower-mass solar-like stars spend more time in the saturated regime than higher-mass solar-like stars, which converge earlier into the unsaturated regime. Moreover, the efficiency of magnetic braking depends on the rotation period: stars born with fast rotation spin down faster than stars born with slow rotation. Eventually, they converge into the same sequence, the unsaturated regime, where they lose angular momentum following the Skumanich law and, thus, gyrochronology becomes valid.

Placing the *Kepler* sample in context, most of the MS stars have already converged into the unsaturated regime. This is not surprising as the *Kepler* sample corresponds to field stars, with a mix of populations of typical ages of several Gyr, and thus stars have had time to spin down. In fact, the transition between the saturated and unsaturated regimes happens at faster rotation rates than the lower edge of the *Kepler* $P_{\rm rot}$ distribution. Both saturated regime and transition are very sparsely populated in the *Kepler* field. Furthermore, this region of the parameter space, particularly $P_{\rm rot} < 7$ days, is found to be dominated by tidally-synchronized binaries, as determined by Simonian et al. (2019) and Angus et al. (2020). Close-in binary candidates identified by Santos et al. (2019, 2021) that survived the selection criteria (Sect. 2) were kept in the *Kepler* MS sample, but they are found to occupy the same region of the parameter space as the tidally-synchronized binaries (with some common targets). It is, thus, unclear whether the surviving *Kepler* rapidly-rotating targets are young solar-like stars still in the saturated regime or tidally-synchronized binaries, which were not identified as such yet.

Figure 2 compares the parameter space of rotation and activity for the X-ray emission sample in Wright et al. (2011, from where we take $T_{\rm eff}$, $P_{\rm rot}$, and color index) and for the *Kepler* MS sample. The left panel show the $P_{\rm rot}$-$T_{\rm eff}$ diagram, while the right panels show the activity-$P_{\rm rot}$ diagram, where F stars were ignored as they are only a few. The color index is used to compute the convective turnover timescale, according to Eq. 10 in Wright et al. (2011), which in turn, together with $P_{\rm rot}$, is used to compute Ro. Ro can vary across different works, depending on the definition of the convective turnover timescale (e.g., the location where it is measured). In this review, we adopt the Ro values as determined by each work, but we focus on the observable $P_{\rm rot}$. Later in this section, we will compare the different Ro values. In what follows, the subscript of Ro indicates to which work they refer, particularly we use the initial of the first author and the year of the publication: e.g., W2011 for Wright et al. (2011).

In Figure 2, we split the X-ray emission sample into saturated and unsaturated regimes according to Wright et al. (2011), with the transition $\mathrm{Ro}_{\rm W2011}$ set at 0.13 (saturated: $\mathrm{Ro}_{\rm W2011} \leq 0.13$; unsaturated: $\mathrm{Ro}_{\rm W2011} > 0.13$). The lower edge of the $P_{\rm rot}$ distribution of the *Kepler* sample lies above the transition between saturated and unsaturated regimes in X-ray luminosity. This comparison emphasizes the fact that, with *Kepler*, we have access mostly to the stars in the unsaturated regime. Interestingly, it is noticeable that the relation between X-ray emission and rotation (right-hand side) shows a change in slope around the intermediate-$P_{\rm rot}$ gap, i.e., where the shape of the *Kepler* contours change. Indeed, one can notice that change in the original figures by Wright et al. (2011). This is also shown in Figure 3, where the color code indicates the distance to the intermediate-$P_{\rm rot}$ gap ($\delta \log P_{\rm rot}$). The top right panel displays the X-ray emission against $\mathrm{Ro}_{\rm W2011}$. Stars in the saturated regime (brown hexagons) are partly omitted to better show the unsaturated regime. Around the intermediate-$P_{\rm rot}$ gap (lighter symbols), there is a decrease in the dispersion compared to the remainder of the unsaturated regime. At $P_{\rm rot}$ longer than the gap ($\delta \log P_{\rm rot} > 0$), stars seem to follow a steeper relation than before. This can be seen through the comparison between the model by Wright et al. (2011, dashed blue line) and the smoothed data (solid red line). In the unsaturated regime, at $\delta \log P_{\rm rot} < 0$, the smoothed line closely follows the model, while deviating at $\delta \log P_{\rm rot} > 0$. Indeed, splitting the unsaturated regime in two and fitting them separately, we find slopes of −1.92 and −2.46 for $\delta \log P_{\rm rot} < 0$ and $\delta \log P_{\rm rot} > 0$, respectively. The behavior change can also be seen in the bottom panels, where particularly for the K stars it is noticeable that stars with $\delta \log P_{\rm rot} < 0$ and $\delta \log P_{\rm rot} > 0$ follow different sequences. This transition in the unsaturated regime was naturally not seen by the authors and is noticed now thanks to the knowledge acquired through the *Kepler* sample, which revealed this intermediate-$P_{\rm rot}$ gap. It is now clear that the unsaturated regime itself presents multiple regimes.

The transition from saturated to unsaturated regime corresponding to the ultra-fast-$P_{\rm rot}$ bimodality can also be found in other magnetic activity proxies besides X-ray emission. For the Pleiades, with an age of ~125 Myr (Stauffer et al., 1998), the saturated and unsaturated regimes are identified, for example, in the photometric magnetic activity measured from K2 light curves (Brown et al., 2021) and in the spot filling factor measured from APOGEE (Apache Point Observatory for Galactic Evolution Experiment) spectra (Cao and Pinsonneault, 2022).

Brown et al. (2021) discovered a new contribution to the stellar brightness variations, the mid-frequency continuum (MFC). The MFC corresponds to an excess of power between ~20 and ~300 μHz in comparison with the models for the acoustic background in the power spectrum, which account for photon-shot noise, activity, and two granulation components. Interestingly, the MFC scales with $\mathrm{Ro}_{\rm B2021}$, suggesting that it is related to stellar magnetism. Given its timescale, the MFC might be related to the supergranular internetwork (see Rincon and Rieutord, 2018 for a review). However, the MFC and the photometric magnetic activity ($\sigma_{\rm H}$, measured as the amplitude of the rotation harmonics, H, in the power spectrum, which is well correlated with $S_{\rm ph}$) do not vary in phase or follow a similar relation with $\mathrm{Ro}_{\rm B2021}$. Brown et al. (2021) found that the MFC also shows two regimes, with the MFC transition taking place

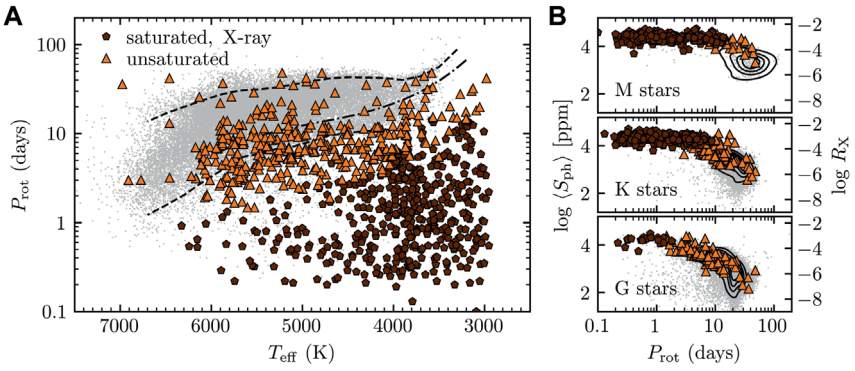

FIGURE 2
Comparison between the rotation and magnetic activity of the *Kepler* sample (gray and black lines) and the X-ray emission sample in (Wright et al. 2011, colored symbols): P_{rot}-T_{eff} diagram **(A)** and activity-P_{rot} diagram per spectral type **(B)**. The saturated and unsaturated regimes identified by Wright et al. (2011) are shown by the brown hexagons and orange triangles respectively. The solid lines in the activity-P_{rot} diagram show the density contours of the *Kepler* sample for reference (see Figure 1). The activity proxy of the *Kepler* sample is S_{ph} (left y-axis), while R_X (right y-axis) corresponds to the ratio between the X-ray and the bolometric luminosities for the X-ray emission sample. The right panels employ dual y-axes, avoiding the need to convert an activity proxy into the other. As the P_{rot} spans roughly the same interval in both samples, we simply align them.

at smaller $\mathrm{Ro}_{\mathrm{B2021}}$ (shorter P_{rot}) than that associated with the ultra-fast-P_{rot} bimodality. This is illustrated in the top panels of Figure 4, where the stars saturated in MFC are shown by the turquoise squares. For the photometric magnetic activity, the transition between the saturated and unsaturated regime (brown hexagons and orange triangles) is consistent with the ultra-fast-P_{rot} bimodality, i.e., with the saturated and unsaturated X-ray regimes. In the top panel of Figure 4, we take the MFC transition from Brown et al. (2021, $\log \mathrm{Ro}_{\mathrm{B2021,MFC}} = -1.65$), while for the photometric activity, we adopt $\log \mathrm{Ro}_{\mathrm{B2021,H}} = -0.7$, which is slightly shifted from the value indicated by the authors ($\log \mathrm{Ro}_{\mathrm{B2021,H}} = -0.5$). This change is motivated by the fact that the stars lying around that $\mathrm{Ro}_{\mathrm{B2021}}$ have already transitioned to the unsaturated regime. T_{eff}, P_{rot}, $\mathrm{Ro}_{\mathrm{B2021}}$, harmonic and MFC amplitudes (σ_H and σ_{MFC}) are adopted from Brown et al. (2021).

In comparison, Cao and Pinsonneault (2022) used APOGEE spectra of the Pleiades cluster to estimate the spot filling factor (f_{spot}), based on the temperature contrast between spots and quiet surroundings. As the activity proxies estimated from K2 light curves and APOGEE spectra are both related to spots, they are expected to show the same behavior. Indeed, that is the case, except with the rotation sequence from Cao and Pinsonneault (2022), which is located at slightly shorter P_{rot} than that from Brown et al. (2021, see middle panel of Figure 4). To split the f_{spot} sample into saturated and unsaturated regimes for Figure 4, we consider the transition at $\log \mathrm{Ro}_{\mathrm{C2022},f_{spot}} = -0.677$ as determined by Cao and Pinsonneault (2022) with their power-law model. The authors identified potential binary or multiple systems, which are neglected for the graphical representation.

The saturated-unsaturated transition associated with the ultra-fast-P_{rot} bimodality can also be seen in the chromospheric activity proxy measured from the emission in the Ca II IRT ($\log R'_{IRT}$). Fritzewski et al. (2021b), Fritzewski et al. (2021a) investigated the rotation and magnetic activity of NGC 3532, whose age is estimated to be around 300 Myr old (Fritzewski et al., 2019). The rotation and magnetic-activity data of this cluster show saturated and unsaturated regimes (bottom panels in Figure 4), consistent with the ultra-fast-P_{rot} bimodality. We adopt T_{eff}, P_{rot}, $\log R'_{IRT}$, and $\mathrm{Ro}_{\mathrm{F2021}}$ from Fritzewski et al. (2021a). According to the authors all the stars with $\mathrm{Ro}_{\mathrm{F2021}} < 0.06$ are in the saturated regime, while stars with $\mathrm{Ro}_{\mathrm{F2021}} > 0.11$ have converged to the rotation sequence. Stars in between would be transitioning from one to the other regime.

Figure 5 compares the activity-Ro diagrams for the stellar samples in Figure 2 and Figure 4. Each panel shows the Ro values as computed in the different works, where the respective best fits are overlaid. Because of the different definitions, the transition from saturated to unsaturated regime happens at different Ro values. However, as seen above, the transitions for the different activity proxies correspond to the same parameter space in terms of the observable P_{rot}. We prefer to focus on P_{rot} here, but when comparing Ro from different works, it is recommended to place them in a uniform scale (e.g., by normalizing to the solar value according to the respective definition).

Reiners et al. (2022) tracked down the transition from the saturated to unsaturated regime in the average magnetic field strength, $\langle B \rangle$, of M dwarfs (and some K) from CARMENES spectra (Figure 6). Similarly, to the magnetic activity proxies above, the transition identified by the authors at their $\mathrm{Ro}_{\mathrm{R2022}} = 1.3$ takes place near the lower edge of the P_{rot} distribution of *Kepler* M dwarfs. For the *Kepler* sample, this edge is not well defined at low T_{eff} due to small sample sizes. Also, the M-dwarf sample of Reiners et al. (2022) is near the location where the gap closes for fully convective stars (at ~3500 K; Lu et al., 2022). Some of the $\langle B \rangle$ measurements are an upper limit. These are mostly located in the more dense region with small $\langle B \rangle$, constituting 37% of the stars with P_{rot} longer than the intermediate-P_{rot} gap. We split the $\langle B \rangle$ unsaturated regime into two according to their location in relation to the intermediate-P_{rot} gap of the *Kepler* sample. In Figure 6 we also show $\log \langle B \rangle$ as a function of $\mathrm{Ro}_{\mathrm{R2022}}$, which was computed using the convective turnover timescale and P_{rot} provided by Reiners et al. (2022).

Gaia also provides photometric data that allow the measurement of rotation periods. Focusing on the targets with a relatively large

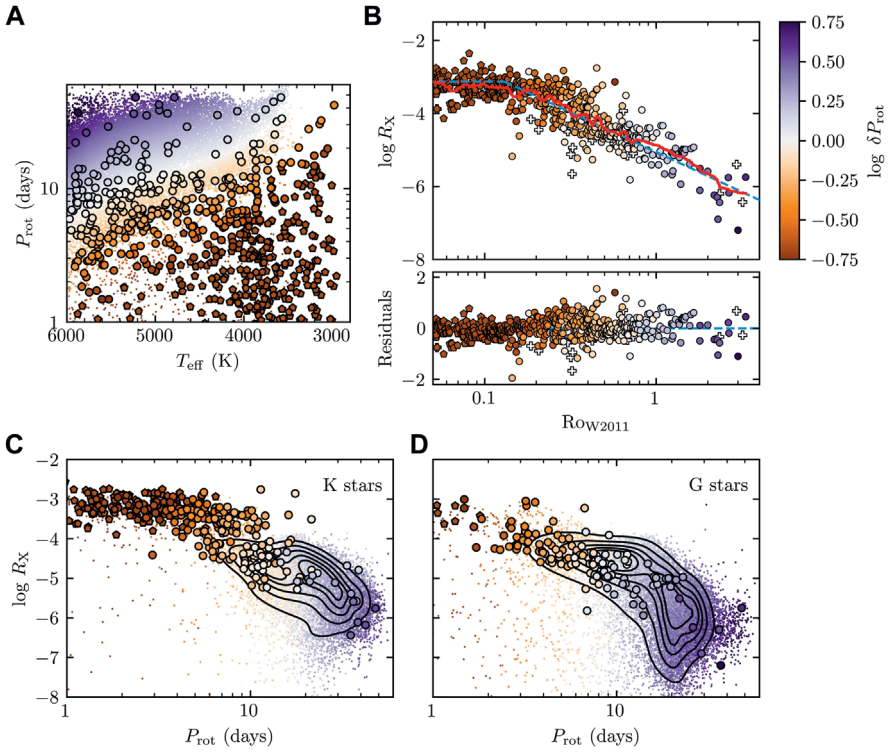

FIGURE 3
Comparison of the *Kepler* and X-ray emission samples, with respect to the intermediate-P_{rot} gap. As in Figure 2, brown hexagons correspond to the stars in the X-ray saturated regime. Dots (*Kepler* sample) and circles (X-ray emission unsaturated regime) are color-coded by their distance to the intermediate-P_{rot} gap ($\delta \log P_{rot}$). The **(A)** shows the P_{rot}-T_{eff} diagram. Note that the axes scale differs from the remainder figures, to better show the relevant parameter space. The **(B)** shows the X-ray emission as a function of the Rossby number, where the white crosses are the F stars, committed elsewhere in this figure. The dashed blue and solid red lines show the model found by Wright et al. (2011) and the smoothed data, respectively. The residuals between the data and the model are presented in the subpanel. The **(C,D)** show the X-ray emission as a function of P_{rot} for the K and G stars (left and right, respectively). The solid lines show the contours for the *Kepler* sample.

number of visits and long temporal coverage, *Gaia* reports P_{rot} and the respective photometric activity proxy (A_{Gaia}, being the amplitude of the rotation signal) for several hundreds of thousands of stars (Lanzafame et al., 2018; Distefano et al., 2023). Indeed, the *Gaia* DR3 sample, with the most reliable P_{rot} estimates, includes of 474,026 stars (Distefano et al., 2023). To complement the rigorous P_{rot} vetting and selection by the authors, which removed evolved stars, we neglect potential binaries (52,933 stars) according to the same criteria used for the *Kepler* sample (Section 2). Figure 7 compares the final *Gaia* (421,093 stars) and *Kepler* samples (34,898 single MS stars). P_{rot} and A_{Gaia} were taken from Distefano et al. (2023), while T_{eff} was taken from Andrae et al. (2023). The parameter spaces probed by Gaia and the *Kepler* barely overlap as noted by Lanzafame et al. (2019) and Distefano et al. (2023). Since Gaia is not very sensitive to long P_{rot} values due to its scanning pattern, all its M stars are still in the saturated regime (Figure 7). *Gaia* G and K stars are spread between both the saturated regime and the "tip" of the unsaturated regime. For those in the unsaturated regime, it is possible to recognize the expected trend with P_{rot} generally decreasing with increasing T_{eff}. *Gaia* also unveiled the existence of stars with P_{rot} < 1 day and very low activity (*ultra-fast rotator branch*), in contrast to the stars in the saturated regime. Lanzafame et al. (2019) hypothesize that stars can either evolve from the saturated regime directly to the unsaturated regime, or to the ultra-fast rotator branch first and from this to the unsaturated regime. This region of the parameter space cannot be explored through the *Kepler* sample, as its majority has already converged to the unsaturated regime.

The comparisons above suggest that the lower edge of the *Kepler* distribution reflects the transition to the unsaturated regime (see also Matt et al., 2015).

4 Intermediate-P_{rot} gap: regimes within the unsaturated regime

The intermediate-P_{rot} gap and the associated P_{rot} bimodality were first discovered in the *Kepler* field of view by McQuillan et al. (2013), McQuillan et al. (2014). One of the original hypotheses was that the P_{rot} bimodality resulted from two different star formation episodes and it was a feature of the *Kepler* field (e.g., McQuillan et al., 2014; Davenport, 2017; Davenport and Covey, 2018). However, since then it has also been recovered in the different campaigns of K2 (Reinhold and Hekker, 2020; Gordon et al., 2021), which focused on different fields of view, and in ground-based data (from the Zwicky Transient Facility survey) covering the full northern hemisphere (Lu et al., 2022). Therefore, these findings suggest that the P_{rot} bimodality and intermediate-P_{rot} gap are linked to stellar evolution.

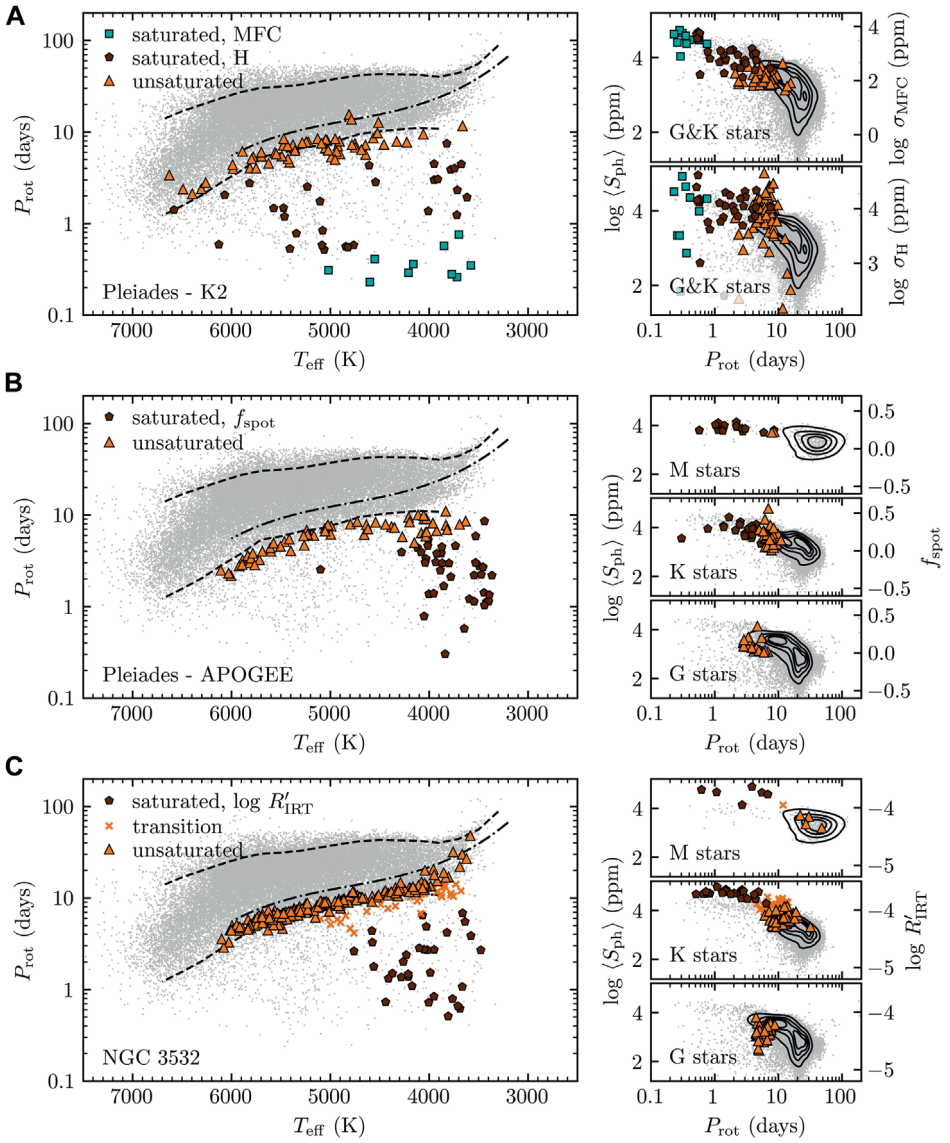

FIGURE 4
Same as Figure 2, but for the Pleiades and NGC 3532. Their activity proxies are σ_H **(A)**, f_{spot} **(B)**, and log R'_{IRT} **(C)**, while σ_{MFC} is the MFC amplitude **(A)**. The top right panels show K and G dwarfs together, while the middle and bottom right panels split the spectral types. The orange and brown symbols correspond to the unsaturated and saturated regimes, respectively. The turquoise shows the MFC-saturated Pleiades members, while the orange crosses show the transitioning NGC 3532 members.

A second hypothesis was postulated by Montet et al. (2017) and Reinhold et al. (2019). These works found evidence for the stars below the intermediate-P_{rot} gap being spot-dominated, while those above the gap being facula-dominated. This led to the proposition that this gap would be related to the transition from the spot-to facula-dominated and it would result from observational biases due to the canceling between dark spots and bright faculae (Reinhold et al., 2019). However, other observational evidence and successful modeling support a third hypothesis.

The hypothesis proposes that this gap has its origin in the core-envelope coupling (McQuillan et al., 2014; Angus et al., 2020; Spada and Lanzafame, 2020; Gordon et al., 2021; Lu et al., 2022), which leads to a stalling in the envelope's spin-down followed by a period of quick evolution once the coupling is completed (Gordon et al., 2021; David et al., 2022). Before and after this transition, stars' envelopes (and thus their surface rotation periods) would follow the Skumanich spin-down law. Starting with a decoupled core-envelope, the surface of the stars below the gap would brake due to magnetized winds. During the coupling between the fast core and the slow envelope, the surface spin-down would stall for a relatively short timescale. Once the coupling is completed, the spin-down would resume. In this light, fully convective stars would not face this transition. Indeed, that was what Lu et al. (2022) found in ground-based photometric data of field stars. The authors retrieve a rotational gap in the partially convective stars, but not for fully convective M dwarfs.

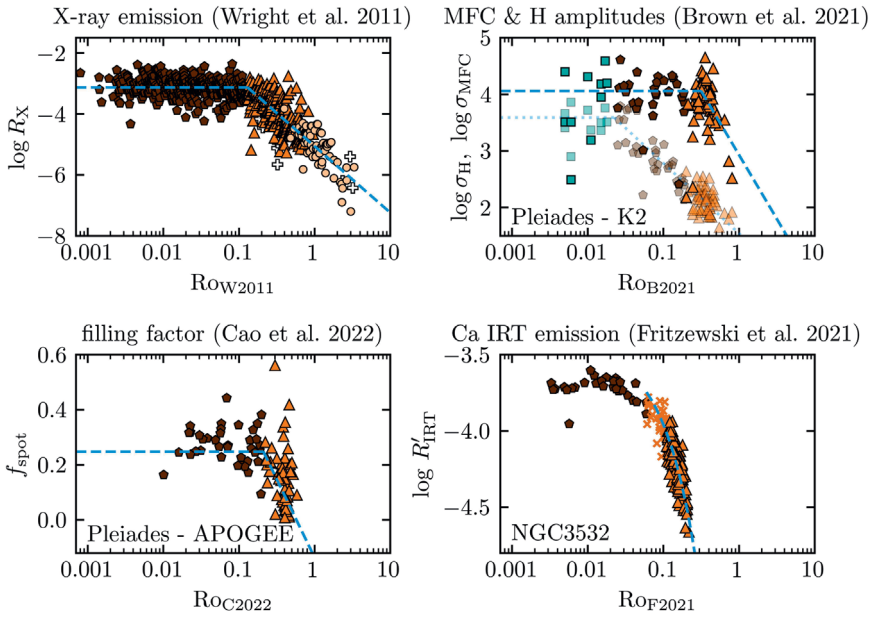

FIGURE 5
Comparison between the activity-Ro relations for samples shown in Figure 2 and Figure 4. The symbols and colors have the same meaning as above, with the addition of the beige circles which represent stars with $\delta \log P_{rot} > 0$, splitting the unsaturated regime in two. Ro is represented according to each work, which is indicated by the subscript. The blue dashed lines show the best fits found in the respective works. In the top right panel, the opaque symbols correspond to the rotation-harmonic component, while the small transparent symbols and dotted line correspond to the MFC. The x-scale is kept the same in all panels to better illustrate the differences in Ro.

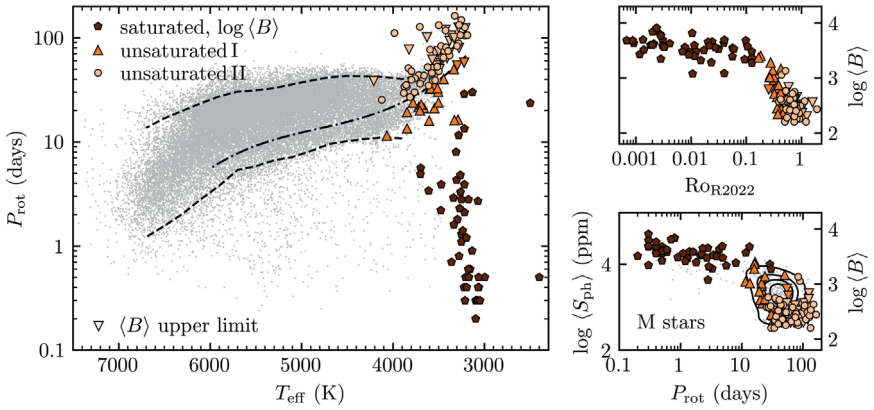

FIGURE 6
Same as Figure 2, but for the M dwarfs in the CARMENES survey. The magnetic activity is measured through the average magnetic field strength ⟨B⟩. The S_{ph}-axis scale is slightly different from the other plots. As in Figure 5, the beige symbols represent stars with $\delta \log P_{rot} > 0$. The downwards triangles identify the stars for which ⟨B⟩ is an upper limit.

The rotational sequence of the 1 Gyr NGC 6811 open cluster is consistent with a stalling in the spin-down of K dwarfs (Curtis et al., 2019), which fits the core-envelope coupling hypothesis. The stalling can be seen through the overlap between the rotational sequences of Praesepe (670 Myr; Douglas et al., 2019) and NGC 6811 in the regime of K-dwarfs (Figure 8; see also Curtis et al., 2019; Bouma et al., 2023), which would not be expected according to the Skumanich spin-down law. The theoretical models by Spada and Lanzafame (2020), which account for a mass-dependent core-envelope coupling timescale, are able to reproduce the observations. In particular, the models match the stalling of the spin-down for K dwarfs around 1 Gyr, consistent with the observations of NGC 6811. The mass-dependent coupling leads to a kink in the rotation sequences at older ages, i.e., the rotation-period sequence is no longer monotonic at these ages. As the coupling timescale increases with decreasing mass (Spada and Lanzafame, 2020), this kink moves towards lower masses with age. This feature is seen in the observational data of older clusters (Figure 8; Meibom et al., 2015; Barnes et al., 2016; Dungee et al., 2022; Bouma et al., 2023).

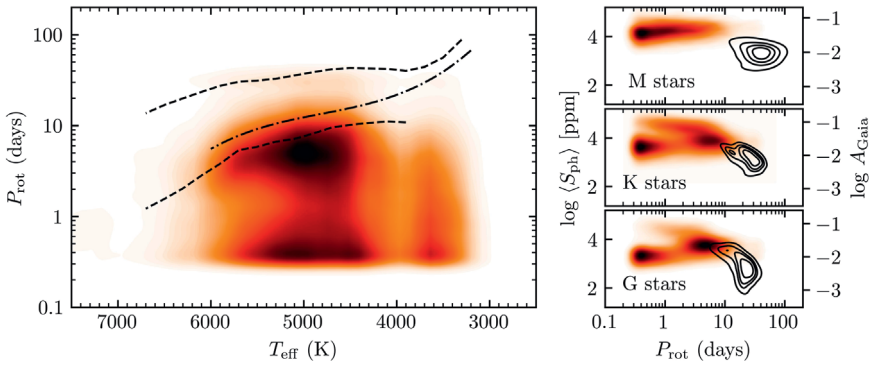

FIGURE 7
Same as in Figure 2, but for the *Gaia* DR3 rotation sample. The *Gaia* sample is shown by the density map, where dark colors correspond to high-density regions. $A_{\rm Gaia}$ is the amplitude of the rotation signal in the *Gaia* photometric data. For the *Kepler* sample, only the limiting lines and contours are shown.

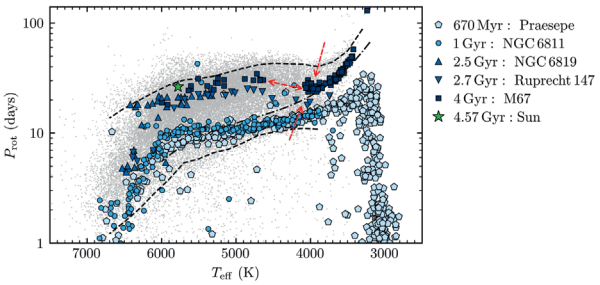

FIGURE 8
Same as the left panel of Figure 2, but for Praesepe, NGC 6811, NGC 6819, Ruprecht 147, M67, and the Sun. The y-axis scale is slightly different from the other plots. The age references are (Bahcall et al., 1995; Jeffries et al., 2013; Barnes et al., 2016; Torres et al., 2020). The one-sided arrows indicate the approximate location of the first deviation to the monotonic behavior in the old clusters' rotation sequence. The double-sided arrow represents the observed increase of $P_{\rm rot}$ with $T_{\rm eff}$, where data is lacking for M67.

Figure 8 compares the rotational sequences of stellar clusters of different ages with the *Kepler* sample. The rotation period and effective temperature for the clusters' members are gathered from different studies (Meibom et al., 2015; Barnes et al., 2016; Godoy-Rivera et al., 2021a; Dungee et al., 2022). Praesepe members are plotted for reference. Most of Praesepe stars with $T_{\rm eff} \gtrsim 3500$ K have already converged to the rotation sequence, while cooler stars have not. The rotation sequence of Praesepe and younger clusters (Figure 4) shows a general monotonic behavior, with $P_{\rm rot}$ decreasing with $T_{\rm eff}$. The remainder of the clusters show evidence of a stalling in the spin-down associated with the intermediate-$P_{\rm rot}$ gap, as discussed above: NGC 6811 partially overlaps with Praesepe; and the older clusters show a kink in the rotation sequence at relatively low temperatures. For the 2.7 Gyr Ruprecht 147, $P_{\rm rot}$ increases with $T_{\rm eff}$ between ~4000 and ~4800 K, while elsewhere it decreases with $T_{\rm eff}$. For the 4 Gyr M67, the rotation sequence starts by decreasing with $T_{\rm eff}$ until ~3900 K, where the behavior inverts. The $P_{\rm rot}$ values at ~3900 K are shorter than those at ~4600 K, suggesting that $P_{\rm rot}$ increases within this interval, despite the lack of data.

Finally, we remind that the imprint of the transition associated with the intermediate-$P_{\rm rot}$ gap can be seen in the relation between X-ray emission and rotation period (Figures 2, 3). Similarly, it can also be identified in the relation between chromospheric emission and rotation (Figure 9, discussed below).

5 Vaughan-Preston gap: discontinuity in the magnetic activity

Focusing on stars with longer periods than the intermediate-$P_{\rm rot}$ gap, another gap has been observed, possibly related to a transition at later stages of stellar evolution. Contrary to the other sections, this transition is not seen in the rotation period. Instead, this transition is seen in the chromospheric activity, where there is a scarceness of stars with intermediary Ca II H & K emission (e.g., Vaughan, 1980; Vaughan and Preston, 1980; Henry et al., 1996; Gomes da Silva et al., 2021). This is known as the Vaughan-Preston (VP) gap. The origin of the VP gap has been contested since its finding: is it of astrophysical origin or an observational bias? Indeed, when investigating larger stellar samples, the gap is not observed anymore (Boro Saikia et al., 2018; Brown et al., 2022). Nevertheless, Brown et al. (2022) concluded that their results are consistent with chromospheric-emission bimodality and associated transitions.

Figure 9 compares the Mount Wilson Observatory (MWO; e.g., Wilson, 1968; Wilson, 1978; Baliunas et al., 1995) sample with the *Kepler* sample: $P_{\rm rot}$, $\mathrm{Ro}_{\rm E2017}$, $\log R'_{\rm HK}$, and (B-V) were adopted from Egeland (2017), see also Lehtinen et al. (2021). For the MWO sample (monitored over two decades), we transform the color index (B-V) into $T_{\rm eff}$, taking into account the metallicity when available. We retrieve metallicity estimates from Valenti and Fischer (2005), Egeland (2017), and APOGEE (Abdurro'ufAccetta et al., 2022) for 60 stars, with a mean value of −0.07 dex. For the remainder, we opt to assume solar metallicity. For the (B-V)-$T_{\rm eff}$ conversion, we use the publicly available routine in `PyAstronomy`[2] (Czesla et al.,

2 https://github.com/sczesla/PyAstronomy

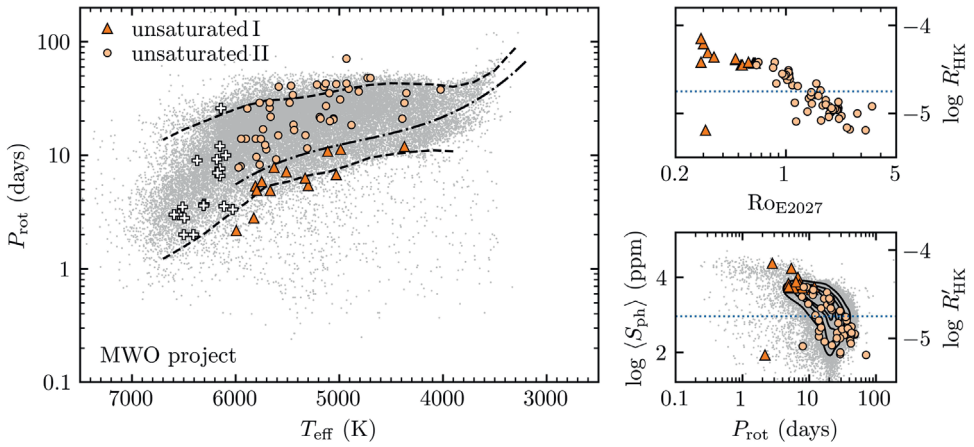

FIGURE 9
Same as Figure 6, but for the MWO stars. The dotted blue line marks the observed VP gap in the chromospheric emission, log $R'_{\rm HK}$. In the bottom right panel, only the G and K *Kepler* dwarfs are shown in gray, with the respective contours. As in Figure 3, the white crosses denote F stars.

2019) based on Ramírez and Meléndez (2005)[3]. One of the targets is ignored because it is outside of the valid parameter space (B-V>1.51). The stars below and above the intermediate-$P_{\rm rot}$ gap (Section 4) are shown in orange and beige, respectively: the dash-dotted line obtained for *Kepler* was used to split the stars. The VP gap located at log $R'_{\rm HK} = -4.75$ is shown by the blue dotted line. As shown by Santos et al. (2021), Santos et al. (2023), there is no evidence of the VP gap in the *Kepler* data, which is several times larger than the ground-based chromospheric emission samples. On the one hand, this could mean that indeed there is an observational bias in the ground-based surveys, and when increasing the sample size, the gap is no longer found. On the other hand, although *Kepler* observations are relatively long-term, their 4-year length is still limiting especially when dealing with a variable property such as magnetic activity. Taking solar data, Santos et al. (2023) showed how the inferences from 4-year observations on magnetic activity and its variation can change over time, depending on the phase of the cycle. The $S_{\rm ph}$ variation strongly depends on the average activity level of the star and on its rotation rate. Consequently, the limiting 4-year monitoring of stars can lead to a smearing of the data points, potentially hiding the possible VP gap. In this case, the large sample size can contribute to a greater concealment.

6 Midlife transition: weakening of the magnetic braking

In recent years, evidence for a possible weakening of the magnetic braking was found (e.g., Metcalfe et al., 2016; van Saders et al., 2016; Hall et al., 2021; Masuda et al., 2022). The surface rotation of the *Kepler* MS asteroseismic targets was found to be too fast in comparison to what was expected given their asteroseismic age (Angus et al., 2015; van Saders et al., 2016). To explain the observations, van Saders et al. (2016) proposed that the magnetic braking would become less efficient at a critical Ro, the so-called weakening of the magnetic braking (WMB). In this case, $P_{\rm rot}$ evolves according to the Skumanich relation until reaching the critical Ro where its evolution is no longer driven by magnetic braking.

The origin of this transition is presently uncertain. One theory suggests that stellar differential rotation weakens around the critical Ro (Metcalfe et al., 2016), disrupting the stellar dynamo process (see the review by Brun and Browning, 2017). In numerical simulations, this can be associated with a shift from solar-like differential rotation, which has a fast equator and slow poles, to solid body or even anti-solar rotation (Brun et al., 2022; Noraz et al., 2022). It has been suggested that this transition could result in a change in magnetic topology from large-scale to small-scale fields (Metcalfe and van Saders, 2017; Metcalfe et al., 2022). However, as the large-scale magnetic field typically governs the efficiency of the magnetic braking (Finley and Matt, 2018), and spectropolarimetric observations have shown it does not abruptly disappear at the critical Ro (See et al., 2019b), it appears more likely that the overall stellar magnetic field strength weakens (Metcalfe et al., 2023). This decrease may also reduce the stellar wind mass-loss rate (Shoda et al., 2023), further weakening the wind braking. In other theories, the evolution of the latitudinal differential rotation is sufficient to stall the rotation-evolution of stars around the critical Ro, due to the active latitudes that couple surface rotation to the stellar wind (Finley and Brun, 2023; Tokuno et al., 2023).

The magnetic cycles of Sun-like stars are also observed to become longer (Soon et al., 1993; Brandenburg et al., 1998; Böhm-Vitense, 2007), with some appearing to lose all cyclic variability akin to the Maunder minimum observed for the Sun (Baum et al., 2022). Interestingly, the Sun is near this critical Ro, which raised the question of whether the Sun could be in transition (Metcalfe et al., 2016) and whether the Maunder Minimum could be a symptom of this. Observations point towards the Sun's magnetic braking being two to three times smaller than required by the Skumanich relation (Finley et al., 2018; Kasper et al., 2021). However, the magnetic

3 https://pyastronomy.readthedocs.io/en/latest/pyaslDoc/aslDoc/aslExt_1Doc/ramirez2005.html

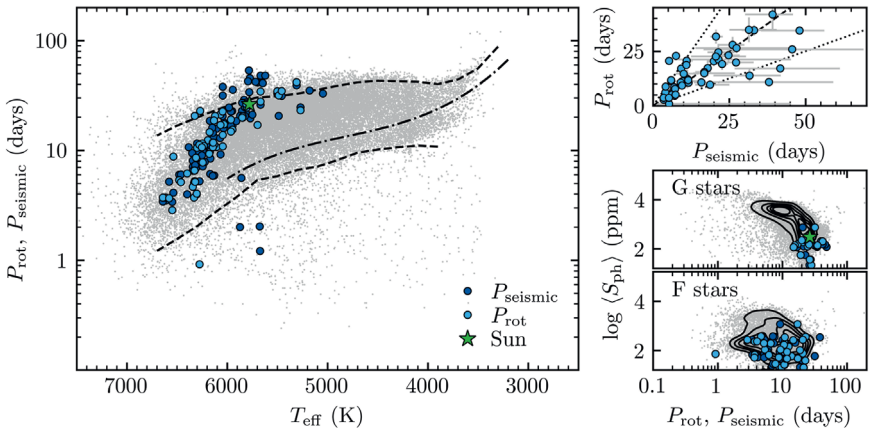

FIGURE 10
Same as Figure 2, but for the *Kepler* asteroseismic sample and the Sun. Dark blue indicates the seismic periods $P_{\rm seismic}$ as determined by Hall et al. (2021), while the light blue indicates the surface periods $P_{\rm rot}$, which were taken by cross-matching with Santos et al. (2019), Santos et al. (2021), from where we also took $S_{\rm ph}$. The top right panel compares the surface ($P_{\rm rot}$) and seismic ($P_{\rm seismic}$) periods for the stars with both estimates (56 stars). The dashed and dotted lines mark the 1:1, 1:2, and 2:1 lines.

braking timescale for the Sun is around 10–100 Myrs, so this disagreement could be explained by long-term variation in solar activity that exceeds the available ~10,000 years of cosmogenic radionuclide records (Finley et al., 2019a).

David et al. (2022) and Metcalfe et al. (2023) identified an overdensity of stars close to the upper edge of the *Kepler* $P_{\rm rot}$ distribution. This might support the WMB as old stars would remain with a largely unchanged surface rotation, which in turn would result in a pileup of stars with different activity levels near this edge. This upper edge is also recovered in van Saders et al. (2019) who simulated the *Kepler* field population using angular momentum evolution models accounting for the WMB. However, we must note that the *Kepler* surface rotation sample does not probe very well this region of the parameter space as it coincides approximately with the current detection limit, which depends on the magnitude (for reference, at *Kepler* magnitude 14, it lies around 100 ppm; Mathur et al., 2023). In both cases, if the stars follow the Skumanich spin-down law or if they face a WMB, stars beyond this point in the main sequence are weakly active and have small amplitude brightness variations due to active regions. Thus, the *Kepler* $P_{\rm rot}$ upper edge can be either the result of one of these effects or the combination of both.

Asteroseismology could come to the rescue as it is easier to detect acoustic oscillations in weakly active stars (e.g., Chaplin et al., 2000; Jiménez et al., 2002; Santos et al., 2018; Mathur et al., 2019). This is also illustrated in Figure 10, as the seismic sample tends to be close to the upper edge of $P_{\rm rot}$ distribution with small $S_{\rm ph}$ values. Sadly, the *Kepler* main-sequence asteroseismic sample with a high enough signal-to-noise ratio to measure rotational splittings is relatively small (94 stars of different mass and metallicity). Nevertheless, Hall et al. (2021) was able to retrieve seismic rotation periods, $P_{\rm seismic}$, for this sample confirming that old stars are rotating faster than expected. Therefore, this discrepancy cannot be solely explained by an observational bias in the $P_{\rm rot}$ sample.

Figure 10 compares the *Kepler* seismic-rotation and surface-rotation samples. The 94 stars from Hall et al. (2021) are shown in dark blue, where their rotation period corresponds to that measured through asteroseismology. Cross-matching this sample with Santos et al. (2019), Santos et al. (2021), we find 56 stars (light blue), out of the 94, with measured surface rotation and $S_{\rm ph}$. In the right, only the 56 stars are shown (twice, in light and dark blue), as $S_{\rm ph}$ is not available for the remainder. We opt to show both $P_{\rm rot}$ and $P_{\rm seismic}$ to demonstrate that both sets of measurements occupy the same parameter space. However, we note that there are some discrepancies between the seismic surface rotation periods (top right panel of Figure 10; Hall et al., 2021, see also Benomar et al., 2015; Breton et al., 2023). Some differences are expected, arising from differential rotation, as the observed acoustic modes are most sensitive to the subsurface layers (e.g., Basu et al., 2012; Benomar et al., 2015) and might be sensitive to different latitudes in comparison to the active-region latitudes. Additionally, there are uncertainties inherent to both techniques. While seismic detections are easier for weakly active stars, which tend to be slow rotators, these are associated with small effects on the acoustic modes, hampering the estimation of $P_{\rm seismic}$. Furthermore, mode linewidths increase with effective temperature (e.g., Appourchaux et al., 2012; Appourchaux et al., 2014; Corsaro et al., 2012; Lund et al., 2017), which poses a challenge because, depending on their values, they can lead to an overlap between azimuthal components, preventing constraints on $P_{\rm seismic}$. There is also a correlation between rotational splitting and inclination angle (e.g., Ballot et al., 2006). As our sensitivity to the active latitudes depends on the inclination angle, inclination has an impact on the amplitude of the light curve modulation due to active regions. Nevertheless, the impact on surface rotation estimate should not be significant. Surface rotation measurements can also be biased toward the half of the true $P_{\rm rot}$ (e.g., McQuillan et al., 2013; McQuillan et al., 2014), but this corresponds to a small percentage of the targets and efforts were made to avoid such misestimations (Santos et al., 2019; Santos et al., 2021; Breton et al., 2021). Finally, photometric pollution by nearby stars can also influence the $P_{\rm rot}$ estimate.

While, as described above, there is evidence supporting the WMB, we emphasize that this regime is at the *Kepler* detection

limit of the surface rotation and that the seismic sample is relatively small. Factors such as the spectral type (many are F stars, with thin convective layers), differential rotation, active latitudes, and chemical composition (see also Claytor et al., 2020) can impact rotation and magnetic-activity evolution. Based on ground-based spectroscopic data of solar twins, Lorenzo-Oliveira et al. (2019) concluded that their results favor a gradual rotation evolution, rather than a broken spin-down law. Future observations are needed to shed light on the evolution of these properties beyond the middle of the star's lifetime.

7 Conclusions and perspectives

Undoubtedly pivotal for exoplanetary and stellar physics, with the end of its second life–the K2 mission–, *Kepler* concluded its operations in the fall of 2018. Despite this, to this day, *Kepler* data continue to be the focal point of numerous studies, consistently contributing to significant discoveries in the field. Considering stellar rotation and magnetic activity, CoRoT (Baglin et al., 2006) had already provided an important sneak-peak into the potential of space-based photometry (e.g., García et al., 2010; Affer et al., 2012). But *Kepler* allowed us to investigate for the first time the rotation and magnetic activity of tens of thousands of solar-like stars. In particular, despite its observational limitations, *Kepler* extended the number of old weakly active stars, like the Sun, with measured rotation and magnetic activity.

In this review, concerning *Kepler*, we focused mostly on the information from the rotation modulation and briefly on asteroseismic inferences. However, it is important to acknowledge that flares can also provide information on the magnetic activity of stars and the environment around them (e.g., Davenport, 2016; Notsu et al., 2019; Yang and Liu, 2019). We place the *Kepler* sample in the context of established or potential transitions in the evolution of rotation and magnetic activity of MS solar-like stars. *Kepler* revealed two unexpected transitions: the intermediate-P_{rot} gap and the WMB. The former is thought to be a transition in the stellar evolution related to the core-envelope coupling, while the physical mechanisms driving the latter are still under debate. One of the main reasons for this debate arises from observational limitations, because of the small number of stars in this regime with measured rotation periods, as these stars are weakly active and below the photometric threshold detection.

Stars are born with strong magnetic activity and rapid rotation rates. As they spin down due to magnetized winds, they eventually converge onto a narrow rotation sequence, transitioning from a saturated regime to an unsaturated regime in magnetic activity. *Kepler* however did not probe the saturated regime well, as most of its stars are relatively old. The transition between saturated and unsaturated regimes coincides roughly with the lower edge of the *Kepler* P_{rot} distribution ($P_{rot} \sim 8$ days at $T_{eff} = 5000$ K).

The unsaturated regime itself splits into different regimes separated by the intermediate-P_{rot} gap ($P_{rot} \sim 12$ days at $T_{eff} = 5000$ K). Currently, the most plausible hypothesis for this observed transition is the core-envelope coupling. This coupling would momentarily stall the surface spin-down due to the angular momentum transfer between the fast-rotating core and the slow-rotating envelope. This transition can also be noticed in the X-ray emission sample in Wright et al. (2011), which was not established before.

In ground-based data, evidence of a possible gap or transition at intermediate magnetic activity has also been found, corresponding to the Vaughan-Preston (VP) gap ($P_{rot} \sim 30$ days at $T_{eff} = 5000$ K). Although there is no evidence of the VP gap in *Kepler* data, it cannot be discarded. On one hand, *Kepler* could support the case for observational bias and the nonexistence of such a gap. On the other hand, the 4-year timespan of *Kepler* observations may be insufficient to fully cover magnetic cycles, especially of solar analogs, leading to a cumulative dispersion that may be enough to conceal the VP gap. This shows the need for longer-term observations to reach a more complete knowledge of the magnetic activity.

The *Kepler* rotation distribution is characterized by a well-defined upper edge ($P_{rot} \sim 40$ days at $T_{eff} = 5000$ K), with the Sun lying near this edge. In recent years, signs of a change in stellar evolution around this edge have been found in seismic observations of solar-like stars, leading to the postulation of the weakening of magnetic braking (WMB). However, the WMB is still under debate, due to observational limitations arising from the hard-to-detect small-amplitude signals. In addition, instrumental artifacts hamper the recovery of rotation periods for slow rotators (e.g., Breton et al., 2021; Santos et al., 2021). If these artifacts can be better mitigated, it will be possible to extend the number of detections in this regime.

This review also shows that the observed behavior of the different activity proxies is similar. In spite of being sensitive to different layers of the stellar atmosphere and different magnetic features, the activity proxies still relate to each other. As a consequence, the well-established transitions in the stellar evolution are found in all. This also reinforces the validity of photometry to measure and investigate magnetic activity.

Gaia has prompted an extraordinary expansion of the number of stars with known rotation and magnetic activity proxies, allowing these properties to be measured for several hundreds of thousands of stars. However, the parameter spaces of *Kepler* and *Gaia* samples do not overlap significantly. Indeed they are complementary: with *Gaia* it is possible to investigate young ultra-fast rotators, which were mostly absent from *Kepler* data. *Gaia* rotation sample yielded the discovery of ultra-fast rotators with unexpected weak magnetic activity. Furthermore, as can be seen above, it is also possible that some of the *Gaia* stars are crossing the intermediate-P_{rot} gap. Thus, in spite of the small sample size in this region of the parameter space, *Gaia* might also provide insights into this transition.

Currently, NASA's TESS (Transiting Exoplanet Survey Satellite; Ricker et al., 2014) is mostly sensitive to the fast strongly active rotators. Nevertheless, future TESS extended missions can expand the reach of this mission, but the photometric precision still will not allow the detection of small amplitude signals.

Future ESA's PLATO (PLAnetary Transits and Oscillations of stars; Rauer et al., 2014) mission, planned to be launched in 2026, will observe stars with high precision and continuously for at least 2 years. PLATO is expected to greatly increase the number of MS solar-like stars and subgiants with seismic detections. The relatively long-term observations will also allow us to measure rotation and magnetic activity both from rotational modulation due to active regions and from asteroseismology. However, as discussed above, one can argue that observations longer than 2 years are needed to provide a better characterization of magnetic activity. Still, thanks

to its high precision, PLATO will be crucial in expanding the observational limit towards more weakly active slower rotators, moving the upper edge of the observed P_{rot} distribution towards longer P_{rot}, which is currently a major challenge in the field. This will provide more information on the rotation and magnetic-activity evolution beyond the age of the Sun, particularly in the regime of the proposed WMB. PLATO is also expected to increase the overlap between seismic and surface rotation samples, both by increasing seismic detections with high SNR and by pushing the detection limit of surface rotation. This overlap will provide complementary information about the stars, particularly accurate ages and different measures of magnetic activity and rotation. This will greatly improve our understanding of stellar evolution and also differential rotation. Moreover, PLATO will observe bright stars, which is a clear advantage in relation to *Kepler*, meaning that complementary ground-based spectroscopic observations will also be possible. This will allow having independent constraints on rotation and magnetic activity, as well as better characterization of the atmospheric parameters of the stars, namely, effective temperature and metallicity. Particularly, better metallicity measurements will help to improve our knowledge of the impact of chemical composition on the magnetic-activity and rotation evolution.

Having observations in different wavelengths will also bring complementary information on the magnetic activity in the different layers of the stellar atmosphere. Furthermore, while dark spots dominate in the passband of the photometric missions mentioned above at the rotation timescale (Shapiro et al., 2016; Li and Basri, 2024), in other wavelengths the bright facula or plage become the most prevalent. As these bright features live longer than spots, they have the potential to produce more stable signals. Therefore, moving away from the optical can increase the rotation yields for stars like the Sun and older (Li and Basri, 2024). Again, this will be particularly important to investigate the WMB and understand the evolution beyond the solar age. Still, long-term observations are required to properly characterize magnetic activity.

PLATO will also be important to investigate the existence of the VP gap, however, the smearing effect described above can be worse in the case of the 2-year observations (in comparison to the *Kepler* 4-year observations). PLATO will also provide more observations for stars around the intermediate-P_{rot} gap and perhaps provide better age constraints for these than what we had before. This can help us to better depict and understand the transition associated with this gap.

One of the most relevant applications of rotation and magnetic activity is age-dating stars. Asteroseismology provides the most precise way to estimate stellar ages, but it is available for a small number of stars. For example, magnetic activity is known to suppress the already small amplitudes of acoustic modes, making seismic detections not possible for relatively high activity levels. In contrast, the detection and characterization of rotation modulation thanks to active regions is easier for such active stars. In principle, this would allow us to provide stellar ages for a large number of stars through gyrochronology, magnetochronology, and/or gyromagnetochronology. However, one needs to better understand the evolution of rotation and magnetic activity. Therefore, unless we understand (or at the very least calibrate) all of these transitions discussed above, the power of age-dating using rotation and magnetic-activity proxies is heavily endangered (e.g., Silva-Beyer et al., 2023). Furthermore, a better understanding of stellar magnetism is also important for exoplanetary physics. Magnetic activity and rotation can disguise or even mimic planetary signals, hampering the detection and characterization of planets (e.g., Queloz et al., 2001; Oshagh et al., 2013; Meunier et al., 2020). Also, these stellar properties have a significant impact on the habitability of the planets, leading for example, to the loss of their atmospheres and shaping the orbital architecture of the systems (e.g., Kaltenegger, 2017; Strugarek, 2018; Owen, 2019). This also reinforces the need for reliable stellar ages, including those determined from rotation and/or magnetic activity, as they will shed light on the evolution of the planetary systems and on the evolution of exoplanet atmospheres.

Author contributions

ÂRGS: Conceptualization, Formal Analysis, Writing–original draft. DG-R: Formal Analysis, Writing–review and editing. AJF: Writing–original draft. SM: Conceptualization, Writing–review and editing. RAG: Conceptualization, Writing–review and editing. SNB: Writing–review and editing. A-MB: Conceptualization, Writing–review and editing.

Funding

The author(s) declare financial support was received for the research, authorship, and/or publication of this article. This work was supported by Fundação para a Ciência e a Tecnologia (FCT) through national funds and by Fundo Europeu de Desenvolvimento Regional (FEDER) through COMPETE2020–Programa Operacional Competitividade e Internacionalização by these grants: UIDB/04434/2020 (DOI: 10.54499/UIDB/04434/2020), UIDP/04434/2020 (DOI: 10.54499/UIDP/04434/2020), & 2022.03993.PTDC (DOI: 10.54499/2022.03993.PTDC). ARGS acknowledges the support from the FCT through the work contract No. 2020.02480.CEECIND/CP1631/CT0001. DG-R and SM acknowledge support from the Spanish Ministry of Science and Innovation (MICINN) grant no. PID2019-107187GB-I00. AJF acknowledges support from the European Research Council (ERC) under the European Union's Horizon 2020 research and innovation programme (grant agreement No 810218 WHOLESUN). SM acknowledges support from the Spanish Ministry of Science and Innovation (MICINN) with the Ramón y Cajal fellowship no. RYC-2015-17697, PID 2019-107061GB-C66 for PLATO, and through AEI under the Severo Ochoa Centres of Excellence Programme 2020–2023 (CEX2019-000920-S). RAG acknowledges the support from PLATO and GOLF CNES grants. SNB acknowledges support from PLATO ASI-INAF agreement n. 2015-019-R.1-2018. A-MB acknowledges the support from STFC consolidated grant ST/T000252/1.

Conflict of interest

The authors declare that the research was conducted in the absence of any commercial or financial relationships that could be construed as a potential conflict of interest.

Publisher's note

References

Abdurro'uf Accetta, K., Aerts, C., Silva Aguirre, V., Ahumada, R., Ajgaonkar, N., et al. (2022). The seventeenth data Release of the sloan digital sky surveys: complete Release of MaNGA, MaStar, and APOGEE-2 data. *ApJS* 259, 35. doi:10.3847/1538-4365/ac4414

Affer, L., Micela, G., Favata, F., and Flaccomio, E. (2012). The rotation of field stars from CoRoT data. *MNRAS* 424, 11–22. doi:10.1111/j.1365-2966.2012.20802.x

Amard, L., and Matt, S. P. (2020). The impact of metallicity on the evolution of the rotation and magnetic activity of sun-like stars. *ApJ* 889, 108. doi:10.3847/1538-4357/ab6173

Amard, L., Roquette, J., and Matt, S. P. (2020). Evidence for metallicity-dependent spin evolution in the Kepler field. *MNRAS* 499, 3481–3493. doi:10.1093/mnras/staa3038

Andrae, R., Fouesneau, M., Sordo, R., Bailer-Jones, C. A. L., Dharmawardena, T. E., Rybizki, J., et al. (2023). Gaia data Release 3. Analysis of the Gaia BP/RP spectra using the general stellar parameterizer from photometry. *A&A* 674, A27. doi:10.1051/0004-6361/202243462

Angus, R., Aigrain, S., Foreman-Mackey, D., and McQuillan, A. (2015). Calibrating gyrochronology using Kepler asteroseismic targets. *MNRAS* 450, 1787–1798. doi:10.1093/mnras/stv423

Angus, R., Beane, A., Price-Whelan, A. M., Newton, E., Curtis, J. L., Berger, T., et al. (2020). Exploring the evolution of stellar rotation using galactic kinematics. *AJ* 160, 90. doi:10.3847/1538-3881/ab91b2

Appourchaux, T., Antia, H. M., Benomar, O., Campante, T. L., Davies, G. R., Handberg, R., et al. (2014). Oscillation mode linewidths and heights of 23 main-sequence stars observed by Kepler. *A&A* 566, A20. doi:10.1051/0004-6361/201323317

Appourchaux, T., Benomar, O., Gruberbauer, M., Chaplin, W. J., García, R. A., Handberg, R., et al. (2012). Oscillation mode linewidths of main-sequence and subgiant stars observed by Kepler. *A&A* 537, A134. doi:10.1051/0004-6361/201118496

Baglin, A., Auvergne, M., Barge, P., Deleuil, M., Catala, C., Michel, E., et al. (2006). "Scientific objectives for a minisat: CoRoT," in *Proceedings of "the CoRoT mission pre-launch status - stellar seismology and planet finding" (ESA SP-1306)*. Editors M. Fridlund, A. Baglin, J. Lochard, and L. Conroy, 1306, 33.

Bahcall, J. N., Pinsonneault, M. H., and Wasserburg, G. J. (1995). Solar models with helium and heavy-element diffusion. *RMP* 67, 781–808. doi:10.1103/RevModPhys.67.781

Baliunas, S. L., Donahue, R. A., Soon, W. H., Horne, J. H., Frazer, J., Woodard-Eklund, L., et al. (1995). Chromospheric variations in main-sequence stars. *ApJ* 438, 269–287. doi:10.1086/175072

Ballot, J., García, R. A., and Lambert, P. (2006). Rotation speed and stellar axis inclination from p modes: how CoRoT would see other suns. *MNRAS* 369, 1281–1286. doi:10.1111/j.1365-2966.2006.10375.x

Balona, L. A. (2015). Flare stars across the H-R diagram. *MNRAS* 447, 2714–2725. doi:10.1093/mnras/stu2651

Balona, L. A. (2019). Evidence for spots on hot stars suggests major revision of stellar physics. *MNRAS* 490, 2112–2116. doi:10.1093/mnras/stz2808

Barnes, S. A. (2003a). A connection between the morphology of the X-ray emission and rotation for solar-type stars in open clusters. *ApJL* 586, L145–L147. doi:10.1086/374681

Barnes, S. A. (2003b). On the rotational evolution of solar- and late-type stars, its magnetic origins, and the possibility of stellar gyrochronology. *ApJ* 586, 464–479. doi:10.1086/367639

Barnes, S. A. (2007). Ages for illustrative field stars using gyrochronology: viability, limitations, and errors. *ApJ* 669, 1167–1189. doi:10.1086/519295

Barnes, S. A., Weingrill, J., Fritzewski, D., Strassmeier, K. G., and Platais, I. (2016). Rotation periods for cool stars in the 4 Gyr old open cluster M67, the solar-stellar connection, and the applicability of gyrochronology to at least solar age. *ApJ* 823, 16. doi:10.3847/0004-637X/823/1/16

Basri, G., Walkowicz, L. M., Batalha, N., Gilliland, R. L., Jenkins, J., Borucki, W. J., et al. (2010). Photometric variability in kepler target stars: the sun among stars—a first look. *ApJL* 713, L155–L159. doi:10.1088/2041-8205/713/2/L155

Basu, S., Broomhall, A.-M., Chaplin, W. J., and Elsworth, Y. (2012). Thinning of the sun's magnetic layer: the peculiar solar minimum could have been predicted. *ApJ* 758, 43. doi:10.1088/0004-637X/758/1/43

Baum, A. C., Wright, J. T., Luhn, J. K., and Isaacson, H. (2022). Five decades of chromospheric activity in 59 sun-like stars and new maunder minimum candidate hd 166620. *AJ* 163, 183. doi:10.3847/1538-3881/ac5683

Bazot, M., Benomar, O., Christensen-Dalsgaard, J., Gizon, L., Hanasoge, S., Nielsen, M., et al. (2019). Latitudinal differential rotation in the solar analogues 16 Cygni A and B. *A&A* 623, A125. doi:10.1051/0004-6361/201834594

Benomar, O., Bazot, M., Nielsen, M. B., Gizon, L., Sekii, T., Takata, M., et al. (2018). Asteroseismic detection of latitudinal differential rotation in 13 Sun-like stars. *Science* 361, 1231–1234. doi:10.1126/science.aao6571

Benomar, O., Takata, M., Shibahashi, H., Ceillier, T., and García, R. A. (2015). Nearly uniform internal rotation of solar-like main-sequence stars revealed by space-based asteroseismology and spectroscopic measurements. *MNRAS* 452, 2654–2674. doi:10.1093/mnras/stv1493

Böhm-Vitense, E. (2007). Chromospheric activity in G and K main-sequence stars, and what it tells us about stellar dynamos. *ApJ* 657, 486–493. doi:10.1086/510482

Bonanno, A., and Corsaro, E. (2022). On the origin of the dichotomy of stellar activity cycles. *ApJ* 939, L26. doi:10.3847/2041-8213/ac9c05

Boro Saikia, S., Marvin, C. J., Jeffers, S. V., Reiners, A., Cameron, R., Marsden, S. C., et al. (2018). Chromospheric activity catalogue of 4454 cool stars. Questioning the active branch of stellar activity cycles. *A&A* 616, A108. doi:10.1051/0004-6361/201629518

Borucki, W. J., Koch, D., Basri, G., Batalha, N., Brown, T., Caldwell, D., et al. (2010). Kepler planet-detection mission: introduction and first results. *Science* 327, 977–980. doi:10.1126/science.1185402

Bouma, L. G., Palumbo, E. K., and Hillenbrand, L. A. (2023). The empirical limits of gyrochronology. *ApJ* 947, L3. doi:10.3847/2041-8213/acc589

Brandenburg, A., Saar, S. H., and Turpin, C. R. (1998). Time evolution of the magnetic activity cycle period. *ApJL* 498, L51–L54. doi:10.1086/311297

Breton, S. N., Dhouib, H., García, R. A., Brun, A. S., Mathis, S., Pérez Hernández, F., et al. (2023). In search of gravity mode signatures in main sequence solar-type stars observed by Kepler. *A&A* 679, A104. doi:10.1051/0004-6361/202346601

Breton, S. N., Santos, A. R. G., Bugnet, L., Mathur, S., García, R. A., and Pallé, P. L. (2021). ROOSTER: a machine-learning analysis tool for Kepler stellar rotation periods. *A&A* 647, A125. doi:10.1051/0004-6361/202039947

Broomhall, A.-M., Chaplin, W. J., Elsworth, Y., and Simoniello, R. (2012). Quasi-biennial variations in helioseismic frequencies: can the source of the variation be localized? *MNRAS* 420, 1405–1414. doi:10.1111/j.1365-2966.2011.20123.x

Broomhall, A.-M., Chatterjee, P., Howe, R., Norton, A. A., and Thompson, M. J. (2014). The sun's interior structure and dynamics, and the solar cycle. *Space Sci. Rev.* 186, 191–225. doi:10.1007/s11214-014-0101-3

Brown, E. L., Jeffers, S. V., Marsden, S. C., Morin, J., Boro Saikia, S., Petit, P., et al. (2022). Linking chromospheric activity and magnetic field properties for late-type dwarf stars. *MNRAS* 514, 4300–4319. doi:10.1093/mnras/stac1291

Brown, T. M. (2014). The metastable dynamo model of stellar rotational evolution. *ApJ* 789, 101. doi:10.1088/0004-637X/789/2/101

Brown, T. M., García, R. A., Mathur, S., Metcalfe, T. S., and Santos, A. R. G. (2021). Brightness fluctuation spectra of sun-like stars. I. The mid-frequency continuum. *ApJ* 916, 66. doi:10.3847/1538-4357/ac0635

Brun, A. S., and Browning, M. K. (2017). Magnetism, dynamo action and the solar-stellar connection. *Living Rev. Sol. Phys.* 14, 4. doi:10.1007/s41116-017-0007-8

Brun, A. S., Strugarek, A., Noraz, Q., Perri, B., Varela, J., Augustson, K., et al. (2022). Powering stellar magnetism: energy transfers in cyclic dynamos of sun-like stars. *ApJ* 926, 21. doi:10.3847/1538-4357/ac469b

Cao, L., and Pinsonneault, M. H. (2022). Star-spots and magnetism: testing the activity paradigm in the Pleiades and M67. *MNRAS* 517, 2165–2189. doi:10.1093/mnras/stac2706

Ceillier, T., Tayar, J., Mathur, S., Salabert, D., García, R. A., Stello, D., et al. (2017). Surface rotation of Kepler red giant stars. *A&A* 605, A111. doi:10.1051/0004-6361/201629884

Chaplin, W. J., Bedding, T. R., Bonanno, A., Broomhall, A.-M., García, R. A., Hekker, S., et al. (2011). Evidence for the impact of stellar activity on the detectability of solar-like oscillations observed by kepler. *ApJL* 732, L5. doi:10.1088/2041-8205/732/1/L5

Chaplin, W. J., Elsworth, Y., Isaak, G. R., Miller, B. A., and New, R. (2000). Variations in the excitation and damping of low- solar p modes over the solar activity cycle. *MNRAS* 313, 32–42. doi:10.1046/j.1365-8711.2000.03176.x

Chaplin, W. J., Elsworth, Y., Isaak, G. R., Miller, B. A., and New, R. (2004). The solar cycle as seen by low-ℓ p-mode frequencies: comparison with global and decomposed activity proxies. *MNRAS* 352, 1102–1108. doi:10.1111/j.1365-2966.2004.07998.x

Claytor, Z. R., van Saders, J. L., Cao, L., Pinsonneault, M. H., Teske, J., and Beaton, R. L. (2023). TESS stellar rotation up to 80 days in the southern continuous viewing zone. *ApJ* 962, 47. doi:10.3847/1538-4357/ad159a

Claytor, Z. R., van Saders, J. L., Santos, A. R. G., García, R. A., Mathur, S., Tayar, J., et al. (2020). Chemical evolution in the milky way: rotation-based ages for APOGEE-kepler cool dwarf stars. *ApJ* 888, 43. doi:10.3847/1538-4357/ab5c24

Corsaro, E., Stello, D., Huber, D., Bedding, T. R., Bonanno, A., Brogaard, K., et al. (2012). Asteroseismology of the open clusters NGC 6791, NGC 6811, and NGC 6819 from 19 Months of kepler photometry. *ApJ* 757, 190. doi:10.1088/0004-637X/757/2/190

Curtis, J. L., Agüeros, M. A., Douglas, S. T., and Meibom, S. (2019). A temporary epoch of stalled spin-down for low-mass stars: insights from NGC 6811 with Gaia and kepler. *ApJ* 879, 49. doi:10.3847/1538-4357/ab2393

Czesla, S., Schröter, S., Schneider, C. P., Huber, K. F., Pfeifer, F., Andreasen, D. T., et al. (2019). *PyA: Python astronomy-related packages*.

Davenport, J. R. A. (2016). The kepler catalog of stellar flares. *ApJ* 829, 23. doi:10.3847/0004-637X/829/1/23

Davenport, J. R. A. (2017). Rotating stars from kepler observed with Gaia DR1. *ApJ* 835, 16. doi:10.3847/1538-4357/835/1/16

Davenport, J. R. A., and Covey, K. R. (2018). Rotating stars from kepler observed with Gaia DR2. *ApJ* 868, 151. doi:10.3847/1538-4357/aae842

David, T. J., Angus, R., Curtis, J. L., van Saders, J. L., Colman, I. L., Contardo, G., et al. (2022). Further evidence of modified spin-down in sun-like stars: pileups in the temperature-period distribution. *ApJ* 933, 114. doi:10.3847/1538-4357/ac6dd3

Davies, G. R., Chaplin, W. J., Farr, W. M., García, R. A., Lund, M. N., Mathis, S., et al. (2015). Asteroseismic inference on rotation, gyrochronology and planetary system dynamics of 16 Cygni. *MNRAS* 446, 2959–2966. doi:10.1093/mnras/stu2331

Distefano, E., Lanzafame, A. C., Brugaletta, E., Holl, B., Lanza, A. F., Messina, S., et al. (2023). Gaia Data Release 3. Rotational modulation and patterns of colour variation in solar-like variables. *A&A* 674, A20. doi:10.1051/0004-6361/202244178

Donati, J. F., and Brown, S. F. (1997). Zeeman-Doppler imaging of active stars. V. Sensitivity of maximum entropy magnetic maps to field orientation. *A&A* 326, 1135–1142.

Douglas, S. T., Curtis, J. L., Agüeros, M. A., Cargile, P. A., Brewer, J. M., Meibom, S., et al. (2019). K2 rotation periods for low-mass hyads and a quantitative comparison of the distribution of slow rotators in the hyades and Praesepe. *ApJ* 879, 100. doi:10.3847/1538-4357/ab2468

Dungee, R., van Saders, J., Gaidos, E., Chun, M., García, R. A., Magnier, E. A., et al. (2022). A 4 Gyr M-dwarf gyrochrone from CFHT/MegaPrime monitoring of the open cluster M67. *ApJ* 938, 118. doi:10.3847/1538-4357/ac90be

Egeland, R. (2017). "Long-term variability of the sun in the context of solar-analog stars," (United States: Montana state university). Ph.D. Thesis.

Elsworth, Y., Howe, R., Isaak, G. R., McLeod, C. P., and New, R. (1990). Variation of low-order acoustic solar oscillations over the solar cycle. *Nature* 345, 322–324. doi:10.1038/345322a0

Findeisen, K., Hillenbrand, L., and Soderblom, D. (2011). Stellar activity in the broadband ultraviolet. *AJ* 142, 23. doi:10.1088/0004-6256/142/1/23

Finley, A. J., and Brun, A. S. (2023). Accounting for differential rotation in calculations of the sun's angular momentum-loss rate. *A&A* 674, A42. doi:10.1051/0004-6361/202245642

Finley, A. J., Deshmukh, S., Matt, S. P., Owens, M., and Wu, C.-J. (2019a). Solar angular momentum loss over the past several millennia. *ApJ* 883, 67. doi:10.3847/1538-4357/ab3729

Finley, A. J., Hewitt, A. L., Matt, S. P., Owens, M., Pinto, R. F., and Réville, V. (2019b). Direct detection of solar angular momentum loss with the wind spacecraft. *ApJL* 885, L30. doi:10.3847/2041-8213/ab4ff4

Finley, A. J., and Matt, S. P. (2018). The effect of combined magnetic geometries on thermally driven winds. ii. dipolar, quadrupolar, and octupolar topologies. *ApJ* 854, 78. doi:10.3847/1538-4357/aaaab5

Finley, A. J., Matt, S. P., and See, V. (2018). The effect of magnetic variability on stellar angular momentum loss. I. The solar wind torque during sunspot cycles 23 and 24. *ApJ* 864, 125. doi:10.3847/1538-4357/aad7b6

Fritzewski, D. J., Barnes, S. A., James, D. J., Geller, A. M., Meibom, S., and Strassmeier, K. G. (2019). Spectroscopic membership for the populous 300 Myr-old open cluster NGC 3532. *A&A* 622, A110. doi:10.1051/0004-6361/201833587

Fritzewski, D. J., Barnes, S. A., James, D. J., Järvinen, S. P., and Strassmeier, K. G. (2021a). A detailed understanding of the rotation-activity relationship using the 300 Myr old open cluster NGC 3532. *A&A* 656, A103. doi:10.1051/0004-6361/202140896

Fritzewski, D. J., Barnes, S. A., James, D. J., and Strassmeier, K. G. (2021b). Rotation periods for cool stars in the open cluster NGC 3532. The transition from fast to slow rotation. *A&A* 652, A60. doi:10.1051/0004-6361/202140894

Gaia Collaboration, Arenou, F., Babusiaux, C., Barstow, M. A., Faigler, S., Jorissen, A., et al. (2023). Gaia Data Release 3: stellar multiplicity, a teaser for the hidden treasure. *A&A* 674 (A34). doi:10.1051/0004-6361/202243782

Gaia Collaboration, Vallenari, A., Brown, A. G. A., Prusti, T., de Bruijne, J. H. J., Arenou, F., et al. (2023). Gaia Data Release 3. Summary of the content and survey properties. *A&A* 674, A1. doi:10.1051/0004-6361/202243940

Gaidos, E. J., Henry, G. W., and Henry, S. M. (2000). Spectroscopy and photometry of nearby young solar analogs. *AJ* 120, 1006–1013. doi:10.1086/301488

Gallet, F., and Bouvier, J. (2013). Improved angular momentum evolution model for solar-like stars. *A&A* 556, A36. doi:10.1051/0004-6361/201321302

García, R. A., Ceillier, T., Salabert, D., Mathur, S., van Saders, J. L., Pinsonneault, M., et al. (2014a). Rotation and magnetism of*Kepler*pulsating solar-like stars: towards asteroseismically calibrated age-rotation relations⋆. *A&A* 572, A34. doi:10.1051/0004-6361/201423888

García, R. A., Gourvès, C., Santos, A. R. G., Strugarek, A., Godoy-Rivera, D., Mathur, S., et al. (2023). Stellar spectral-type (mass) dependence of the dearth of close-in planets around fast-rotating stars. Architecture of Kepler confirmed single-exoplanet systems compared to star-planet evolution models. *A&A* 679, L12. doi:10.1051/0004-6361/202346933

García, R. A., Hekker, S., Stello, D., Gutiérrez-Soto, J., Handberg, R., Huber, D., et al. (2011). Preparation of Kepler light curves for asteroseismic analyses. *MNRAS* 414, L6–L10. doi:10.1111/j.1745-3933.2011.01042.x

García, R. A., Mathur, S., Pires, S., Régulo, C., Bellamy, B., Pallé, P. L., et al. (2014b). Impact on asteroseismic analyses of regular gaps in Kepler data. *A&A* 568, A10. doi:10.1051/0004-6361/201323326

García, R. A., Mathur, S., Salabert, D., Ballot, J., Regulo, C., Metcalfe, T. S., et al. (2010). CoRoT reveals a magnetic activity cycle in a sun-like star. *Science* 329, 1032. doi:10.1126/science.1191064

Garraffo, C., Drake, J. J., and Cohen, O. (2016). The missing magnetic morphology term in stellar rotation evolution. *A&A* 595, A110. doi:10.1051/0004-6361/201628367

Garraffo, C., Drake, J. J., Dotter, A., Choi, J., Burke, D. J., Moschou, S. P., et al. (2018). The revolution revolution: magnetic morphology driven spin-down. *ApJ* 862, 90. doi:10.3847/1538-4357/aace5d

Gehan, C., Gaulme, P., and Yu, J. (2022). Surface magnetism of rapidly rotating red giants: single versus close binary stars. *A&A* 668, A116. doi:10.1051/0004-6361/202245083

Gehan, C., Godoy-Rivera, D., and Gaulme, P. (2024). *Magnetic activity of red giants: a near-UV and Hα view, and the enhancing role of tidal interactions*. arXiv. doi:10.48550/arXiv.2401.13549

Gizon, L., Ballot, J., Michel, E., Stahn, T., Vauclair, G., Bruntt, H., et al. (2013). Seismic constraints on rotation of Sun-like star and mass of exoplanet. *Proc. Natl. Acad. Sci.* 110, 13267–13271. doi:10.1073/pnas.1303291110

Gizon, L., and Solanki, S. K. (2003). Determining the inclination of the rotation Axis of a sun-like star. *ApJ* 589, 1009–1019. doi:10.1086/374715

Godoy-Rivera, D., Pinsonneault, M. H., and Rebull, L. M. (2021a). Stellar rotation in the Gaia era: revised open clusters' sequences. *ApJS* 257, 46. doi:10.3847/1538-4365/ac2058

Godoy-Rivera, D., Tayar, J., Pinsonneault, M. H., Rodríguez Martínez, R., Stassun, K. G., van Saders, J. L., et al. (2021b). Testing the limits of precise subgiant characterization with APOGEE and Gaia: opening a window to unprecedented astrophysical studies. *ApJ* 915, 19. doi:10.3847/1538-4357/abf8ba

Gomes da Silva, J., Santos, N. C., Adibekyan, V., Sousa, S. G., Campante, T. L., Figueira, P., et al. (2021). Stellar chromospheric activity of 1674 FGK stars from the AMBRE-HARPS sample. I. A catalogue of homogeneous chromospheric activity. *A&A* 646, A77. doi:10.1051/0004-6361/202039765

Gordon, T. A., Davenport, J. R. A., Angus, R., Foreman-Mackey, D., Agol, E., Covey, K. R., et al. (2021). Stellar rotation in the K2 sample: evidence for modified spin-down. *ApJ* 913, 70. doi:10.3847/1538-4357/abf63e

Gosnell, N. M., Gully-Santiago, M. A., Leiner, E. M., and Tofflemire, B. M. (2022). Observationally constraining the starspot properties of magnetically active M67 sub-subgiant S1063. *ApJ* 925, 5. doi:10.3847/1538-4357/ac3668

Gully-Santiago, M. A., Herczeg, G. J., Czekala, I., Somers, G., Grankin, K., Covey, K. R., et al. (2017). Placing the spotted T tauri star LkCa 4 on an HR diagram. *ApJ* 836, 200. doi:10.3847/1538-4357/836/2/200

Günther, M. N., Zhan, Z., Seager, S., Rimmer, P. B., Ranjan, S., Stassun, K. G., et al. (2020). Stellar flares from the first TESS data Release: exploring a new sample of M dwarfs. *AJ* 159, 60. doi:10.3847/1538-3881/ab5d3a

Hale, G. E., Ellerman, F., Nicholson, S. B., and Joy, A. H. (1919). The magnetic polarity of sun-spots. *ApJ* 49, 153. doi:10.1086/142452

Hall, O. J., Davies, G. R., van Saders, J., Nielsen, M. B., Lund, M. N., Chaplin, W. J., et al. (2021). Weakened magnetic braking supported by asteroseismic rotation rates of Kepler dwarfs. *Nat. Astron.* 5, 707–714. doi:10.1038/s41550-021-01335-x

Hathaway, D. H. (2015). The solar cycle. *Living Rev. Sol. Phys.* 12, 4. doi:10.1007/lrsp-2015-4

Henriksen, A. I., Antoci, V., Saio, H., Cantiello, M., Kjeldsen, H., Kurtz, D. W., et al. (2023). Rotational modulation in A and F stars: magnetic stellar spots or convective core rotation? *MNRAS* 520, 216–232. doi:10.1093/mnras/stad153

Henry, T. J., Soderblom, D. R., Donahue, R. A., and Baliunas, S. L. (1996). A survey of Ca II H and K chromospheric emission in southern solar-type stars. *AJ* 111, 439. doi:10.1086/117796

Howell, S. B., Sobeck, C., Haas, M., Still, M., Barclay, T., Mullally, F., et al. (2014). The K2 mission: characterization and early results. *PASP* 126, 398–408. doi:10.1086/676406

Ilin, E., Schmidt, S. J., Davenport, J. R. A., and Strassmeier, K. G. (2019). Flares in open clusters with K2 . I. M 45 (Pleiades), M 44 (Praesepe), and M 67. *A&A* 622, A133. doi:10.1051/0004-6361/201834400

Ilin, E., Schmidt, S. J., Poppenhäger, K., Davenport, J. R. A., Kristiansen, M. H., and Omohundro, M. (2021). Flares in open clusters with K2. II. Pleiades, hyades, Praesepe, Ruprecht 147, and M 67. *A&A* 645, A42. doi:10.1051/0004-6361/202039198

Jain, K., Tripathy, S. C., and Hill, F. (2009). Solar activity phases and intermediate-degree mode frequencies. *ApJ* 695, 1567–1576. doi:10.1088/0004-637X/695/2/1567

Jeffries, M. W., Jr., Sandquist, E. L., Mathieu, R. D., Geller, A. M., Orosz, J. A., Milliman, K. E., et al. (2013). WOCS 40007: a detached eclipsing binary near the turnoff of the open cluster NGC 6819. *AJ* 146, 58. doi:10.1088/0004-6256/146/3/58

Jenkins, J. M., Caldwell, D. A., Chandrasekaran, H., Twicken, J. D., Bryson, S. T., Quintana, E. V., et al. (2010). Overview of the kepler science processing pipeline. *ApJL* 713, L87–L91. doi:10.1088/2041-8205/713/2/L87

Jiménez, A., Roca Cortés, T., and Jiménez-Reyes, S. J. (2002). Variation of the low-degree solar acoustic mode parameters over the solar cycle. *Sol. Phys.* 209, 247–263. doi:10.1023/A:1021226503589

Jiménez-Reyes, S. J., Régulo, C., Pallé, P. L., and Roca Cortes, T. (1998). Solar activity cycle frequency shifts of low-degree p-modes. *A&A* 329, 1119–1124.

Kaltenegger, L. (2017). How to characterize habitable worlds and signs of life. *ARA&A* 55, 433–485. doi:10.1146/annurev-astro-082214-122238

Karoff, C., Knudsen, M. F., De Cat, P., Bonanno, A., Fogtmann-Schulz, A., Fu, J., et al. (2016). Observational evidence for enhanced magnetic activity of superflare stars. *Nat. Commun.* 7, 11058. doi:10.1038/ncomms11058

Karoff, C., Metcalfe, T. S., Santos, A. R. G., Montet, B. T., Isaacson, H., Witzke, V., et al. (2018). The influence of metallicity on stellar differential rotation and magnetic activity. *ApJ* 852, 46. doi:10.3847/1538-4357/aaa026

Kasper, J., Klein, K., Lichko, E., Huang, J., Chen, C., Badman, S., et al. (2021). Parker solar probe enters the magnetically dominated solar corona. *Phys. Rev. Lett.* 127, 255101. doi:10.1103/physrevlett.127.255101

Katz, D., Sartoretti, P., Guerrier, A., Panuzzo, P., Seabroke, G. M., Thévenin, F., et al. (2023). Gaia Data Release 3. Properties and validation of the radial velocities. *A&A* 674, A5. A5. doi:10.1051/0004-6361/202244220

Kawaler, S. D. (1988). Angular momentum loss in low-mass stars. *ApJ* 333, 236. doi:10.1086/166740

Kiefer, R., Schad, A., Davies, G., and Roth, M. (2017). Stellar magnetic activity and variability of oscillation parameters: an investigation of 24 solar-like stars observed by Kepler. *A&A* 598, A77. doi:10.1051/0004-6361/201628469

Kirk, B., Conroy, K., Prša, A., Abdul-Masih, M., Kochoska, A., Matijevič, G., et al. (2016). Kepler eclipsing binary stars. VII. The catalog of eclipsing binaries found in the entire kepler data set. *AJ* 151, 68. doi:10.3847/0004-6256/151/3/68

Kochukhov, O. (2021). Magnetic fields of M dwarfs. *A&ARv* 29, 1. doi:10.1007/s00159-020-00130-3

Kraft, R. P. (1967). Studies of stellar rotation. V. The dependence of rotation on age among solar-type stars. *ApJ* 150, 551. doi:10.1086/149359

Lanzafame, A. C., Distefano, E., Barnes, S. A., and Spada, F. (2019). Evidence of new magnetic transitions in late-type dwarfs from Gaia DR2. *ApJ* 877, 157. doi:10.3847/1538-4357/ab1aa2

Lanzafame, A. C., Distefano, E., Messina, S., Pagano, I., Lanza, A. F., Eyer, L., et al. (2018). Gaia data Release 2 - rotational modulation in late-type dwarfs. *A&A* 616, A16. doi:10.1051/0004-6361/201833334

Lehtinen, J. J., Käpylä, M. J., Olspert, N., and Spada, F. (2021). A knee point in the rotation-activity scaling of late-type stars with a connection to dynamo transitions. *ApJ* 910, 110. doi:10.3847/1538-4357/abe621

Leighton, R. B. (1959). Observations of solar magnetic fields in plage regions. *ApJ* 130, 366. doi:10.1086/146727

Li, C., and Basri, G. (2024). *Do faculae affect autocorrelation rotation periods in sun-like stars?* arXiv. doi:10.48550/arXiv.2401.13003

Lorenzo-Oliveira, D., Freitas, F. C., Meléndez, J., Bedell, M., Ramírez, I., Bean, J. L., et al. (2018). The solar twin planet search. The age-chromospheric activity relation. *A&A* 619, A73. doi:10.1051/0004-6361/201629294

Lorenzo-Oliveira, D., Meléndez, J., Yana Galarza, J., Ponte, G., dos Santos, L. A., Spina, L., et al. (2019). Constraining the evolution of stellar rotation using solar twins. *MNRAS* 485, L68–L72. doi:10.1093/mnrasl/slz034

Lu, Y., Angus, R., Foreman-Mackey, D., and Hattori, S. (2023). *In this day and age: an empirical gyrochronology relation for partially and fully convective single field stars*. arXiv. doi:10.48550/arXiv.2310.14990

Lu, Y. L., Curtis, J. L., Angus, R., David, T. J., and Hattori, S. (2022). Bridging the gap-the disappearance of the intermediate period gap for fully convective stars, uncovered by new ZTF rotation periods. *AJ* 164, 251. doi:10.3847/1538-3881/ac9bee

Lund, M. N., Silva Aguirre, V., Davies, G. R., Chaplin, W. J., Christensen-Dalsgaard, J., Houdek, G., et al. (2017). Standing on the shoulders of dwarfs: the kepler asteroseismic LEGACY sample. I. Oscillation mode parameters. *ApJ* 835, 172. doi:10.3847/1538-4357/835/2/172

Mamajek, E. E., and Hillenbrand, L. A. (2008). Improved age estimation for solar-type dwarfs using activity-rotation diagnostics. *ApJ* 687, 1264–1293. doi:10.1086/591785

Masuda, K., Petigura, E. A., and Hall, O. J. (2022). Inferring the rotation period distribution of stars from their projected rotation velocities and radii: application to late-F/early-G Kepler stars. *MNRAS* 510, 5623–5638. doi:10.1093/mnras/stab3650

Mathur, S., Claytor, Z. R., Santos, A. R. G., García, R. A., Amard, L., Bugnet, L., et al. (2023). Magnetic activity evolution of solar-like stars. I. S ph-age relation derived from kepler observations. *ApJ* 952, 131. doi:10.3847/1538-4357/acd118

Mathur, S., García, R. A., Ballot, J., Ceillier, T., Salabert, D., Metcalfe, T. S., et al. (2014a). Magnetic activity of F stars observed by Kepler. *A&A* 562, A124. doi:10.1051/0004-6361/201322707

Mathur, S., García, R. A., Bugnet, L., Santos, A. R. G., Santiago, N., and Beck, P. G. (2019). Revisiting the impact of stellar magnetic activity on the detectability of solar-like oscillations by kepler. *FrASS* 6, 46. doi:10.3389/fspas.2019.00046

Mathur, S., Salabert, D., García, R. A., and Ceillier, T. (2014b). Photometric magnetic-activity metrics tested with the Sun: application to Kepler M dwarfs. *JSWSC* 4, A15. doi:10.1051/swsc/2014011

Mathys, G. (2017). Ap stars with resolved magnetically split lines: magnetic field determinations from Stokes I and V spectra. *A&A* 601, A14. doi:10.1051/0004-6361/201628429

Matt, S. P., Brun, A. S., Baraffe, I., Bouvier, J., and Chabrier, G. (2015). The mass-dependence of angular momentum evolution in sun-like stars. *ApJ* 799, L23. doi:10.1088/2041-8205/799/2/L23

McQuillan, A., Aigrain, S., and Mazeh, T. (2013). Measuring the rotation period distribution of field M dwarfs with Kepler. *MNRAS* 432, 1203–1216. doi:10.1093/mnras/stt536

McQuillan, A., Mazeh, T., and Aigrain, S. (2014). Rotation periods of 34,030 kepler main-sequence stars: the full autocorrelation sample. *ApJS* 211, 24. doi:10.1088/0067-0049/211/2/24

Meibom, S., Barnes, S. A., Platais, I., Gilliland, R. L., Latham, D. W., and Mathieu, R. D. (2015). A spin-down clock for cool stars from observations of a 2.5-billion-year-old cluster. *Nature* 517, 589–591. doi:10.1038/nature14118

Metcalfe, T. S., Egeland, R., and van Saders, J. (2016). Stellar evidence that the solar dynamo may Be in transition. *ApJL* 826, L2. doi:10.3847/2041-8205/826/1/L2

Metcalfe, T. S., Finley, A. J., Kochukhov, O., See, V., Ayres, T. R., Stassun, K. G., et al. (2022). The origin of weakened magnetic braking in old solar analogs. *ApJL* 933, L17. doi:10.3847/2041-8213/ac794d

Metcalfe, T. S., Strassmeier, K. G., Ilyin, I. V., van Saders, J. L., Ayres, T. R., Finley, A. J., et al. (2023). Constraints on magnetic braking from the G8 dwarf stars 61 UMa and τ cet. *ApJL* 948, L6. doi:10.3847/2041-8213/acce38

Metcalfe, T. S., and van Saders, J. (2017). Magnetic evolution and the disappearance of sun-like activity cycles. *Sol. Phys.* 292, 126. doi:10.1007/s11207-017-1157-5

Metcalfe, T. S., van Saders, J. L., Basu, S., Buzasi, D., Drake, J. J., Egeland, R., et al. (2021). Magnetic and rotational evolution of ρ CrB from asteroseismology with TESS. *ApJ* 921, 122. doi:10.3847/1538-4357/ac1f19

Meunier, N., Lagrange, A. M., and Borgniet, S. (2020). Activity time series of old stars from late F to early K. V. Effect on exoplanet detectability with high-precision astrometry. *A&A* 644, A77. doi:10.1051/0004-6361/202038710

Montet, B. T., Tovar, G., and Foreman-Mackey, D. (2017). Long-term photometric variability in kepler full-frame images: magnetic cycles of sun-like stars. *ApJ* 851, 116. doi:10.3847/1538-4357/aa9e00

Newton, E. R., Irwin, J., Charbonneau, D., Berlind, P., Calkins, M. L., and Mink, J. (2017). The Hα emission of nearby M dwarfs and its relation to stellar rotation. *ApJ* 834, 85. doi:10.3847/1538-4357/834/1/85

Nielsen, M. B., Gizon, L., Schunker, H., and Karoff, C. (2013). Rotation periods of 12 000 main-sequence Kepler stars: dependence on stellar spectral type and comparison with v sin i observations. *A&A* 557, L10. doi:10.1051/0004-6361/201321912

Nielsen, M. B., Schunker, H., Gizon, L., Schou, J., and Ball, W. H. (2017). Limits on radial differential rotation in Sun-like stars from parametric fits to oscillation power spectra. *A&A* 603, A6. doi:10.1051/0004-6361/201730896

Noraz, Q., Brun, A. S., Strugarek, A., and Depambour, G. (2022). Impact of anti-solar differential rotation in mean-field solar-type dynamos-exploring possible magnetic cycles in slowly rotating stars. *A&A* 658, A144. doi:10.1051/0004-6361/202141946

Notsu, Y., Maehara, H., Honda, S., Hawley, S. L., Davenport, J. R. A., Namekata, K., et al. (2019). Do kepler superflare stars really include slowly rotating sun-like stars?results using APO 3.5 m telescope spectroscopic observations and gaia-DR2 data. *ApJ* 876, 58. doi:10.3847/1538-4357/ab14e6

Noyes, R. W., Hartmann, L. W., Baliunas, S. L., Duncan, D. K., and Vaughan, A. H. (1984). Rotation, convection, and magnetic activity in lower main-sequence stars. *ApJ* 279, 763–777. doi:10.1086/161945

Oláh, K., Kolláth, Z., Granzer, T., Strassmeier, K. G., Lanza, A. F., Järvinen, S., et al. (2009). Multiple and changing cycles of active stars. II. Results. *A&A* 501, 703–713. doi:10.1051/0004-6361/200811304

Oshagh, M., Santos, N. C., Boisse, I., Boué, G., Montalto, M., Dumusque, X., et al. (2013). Effect of stellar spots on high-precision transit light-curve. *ASTRONOMY ASTROPHYSICS* 556, A19. doi:10.1051/0004-6361/201321309

Owen, J. E. (2019). Atmospheric escape and the evolution of close-in exoplanets. *AREPS* 47, 67–90. doi:10.1146/annurev-earth-053018-060246

Pace, G. (2013). Chromospheric activity as age indicator: an L-shaped chromospheric-activity versus age diagram⋆. *A&A* 551, L8. doi:10.1051/0004-6361/201220364

Pallavicini, R., Golub, L., Rosner, R., Vaiana, G. S., Ayres, T., and Linsky, J. L. (1981). Relations among stellar X-ray emission observed from Einstein, stellar rotation and bolometric luminosity. *ApJ* 248, 279–290. doi:10.1086/159152

Pillitteri, I., Micela, G., Damiani, F., and Sciortino, S. (2006). Deep X-ray survey of the young open cluster NGC 2516 with XMM-Newton. *A&A* 450, 993–1004. doi:10.1051/0004-6361:20054003

Pinsonneault, M. H., Kawaler, S. D., Sofia, S., and Demarque, P. (1989). Evolutionary models of the rotating sun. *ApJ* 338, 424. doi:10.1086/167210

Pizzolato, N., Maggio, A., Micela, G., Sciortino, S., and Ventura, P. (2003). The stellar activity-rotation relationship revisited: dependence of saturated and non-saturated X-ray emission regimes on stellar mass for late-type dwarfs. *A&A* 397, 147–157. doi:10.1051/0004-6361:20021560

Ponte, G., Lorenzo-Oliveira, D., Melendez, J., Yana Galarza, J., and Valio, A. (2023). Photometric variations from stellar activity as an age indicator for solar-twins. *MNRAS* 522, 2675–2682. doi:10.1093/mnras/stad1085

Queloz, D., Henry, G. W., Sivan, J. P., Baliunas, S. L., Beuzit, J. L., Donahue, R. A., et al. (2001). No planet for HD 166435. *A&A* 379, 279–287. doi:10.1051/0004-6361:20011308

Ramírez, I., and Meléndez, J. (2005). The effective temperature scale of FGK stars. II. Teff:Color:[Fe/H] calibrations. *ApJ* 626, 465–485. doi:10.1086/430102

Rauer, H., Catala, C., Aerts, C., Appourchaux, T., Benz, W., Brandeker, A., et al. (2014). The PLATO 2.0 mission. *Exp. Astron.* 38, 249–330. doi:10.1007/s10686-014-9383-4

Reiners, A., Shulyak, D., Käpylä, P. J., Ribas, I., Nagel, E., Zechmeister, M., et al. (2022). Magnetism, rotation, and nonthermal emission in cool stars - average magnetic field measurements in 292 M dwarfs. *A&A* 662, A41. doi:10.1051/0004-6361/202243251

Reinhold, T., Bell, K. J., Kuszlewicz, J., Hekker, S., and Shapiro, A. I. (2019). Transition from spot to faculae domination. An alternate explanation for the dearth of intermediate Kepler rotation periods. *A&A* 621, A21. doi:10.1051/0004-6361/201833754

Reinhold, T., and Hekker, S. (2020). Stellar rotation periods from K2 Campaigns 0-18. Evidence for rotation period bimodality and simultaneous variability decrease. *A&A* 635, A43. doi:10.1051/0004-6361/201936887

Reinhold, T., Reiners, A., and Basri, G. (2013). Rotation and differential rotation of active Kepler stars. *A&A* 560, A4. doi:10.1051/0004-6361/201321970

Reinhold, T., Shapiro, A. I., Solanki, S. K., and Basri, G. (2023). New rotation period measurements of 67 163 Kepler stars. *A&A* 678, A24. doi:10.1051/0004-6361/202346789

Réville, V., Brun, A. S., Matt, S. P., Strugarek, A., and Pinto, R. F. (2015). The effect of magnetic topology on thermally driven wind: toward a general formulation of the braking law. *ApJ* 798, 116. doi:10.1088/0004-637X/798/2/116

Ricker, G. R., Winn, J. N., Vanderspek, R., Latham, D. W., Bakos, G. A., Bean, J. L., et al. (2014). "Transiting exoplanet survey satellite (TESS) 9143," in Conference Name: Space Telescopes and Instrumentation 2014: Optical, Infrared, and Millimeter Wave Place. doi:10.1117/12.2063489914320

Rincon, F., and Rieutord, M. (2018). The Sun's supergranulation. *Living Rev. Sol. Phys.* 15, 6. doi:10.1007/s41116-018-0013-5

Saikia, S. B., Lueftinger, T., Jeffers, S., Folsom, C., See, V., Petit, P., et al. (2018). Direct evidence of a full dipole flip during the magnetic cycle of a sun-like star. *A&A* 620, L11. doi:10.1051/0004-6361/201834347

Salabert, D., García, R. A., Beck, P. G., Egeland, R., Pallé, P. L., Mathur, S., et al. (2016). Photospheric and chromospheric magnetic activity of seismic solar analogs: observational inputs on the solar-stellar connection from*Kepler*and Hermes ⋆. *A&A* 596, A31. doi:10.1051/0004-6361/201628583

Salabert, D., García, R. A., Jiménez, A., Bertello, L., Corsaro, E., and Pallé, P. L. (2017). Photospheric activity of the Sun with VIRGO and GOLF. Comparison with standard activity proxies. *A&A* 608, A87. doi:10.1051/0004-6361/201731560

Salabert, D., García, R. A., and Turck-Chièze, S. (2015). Seismic sensitivity to sub-surface solar activity from 18 yr of GOLF/SoHO observations. *A&A* 578, A137. doi:10.1051/0004-6361/201425236

Santos, A. R. G., Breton, S. N., Mathur, S., and García, R. A. (2021). Surface rotation and photometric activity for kepler targets. II. G and F Main-sequence stars and cool subgiant stars. *ApJS* 255, 17. doi:10.3847/1538-4365/ac033f

Santos, A. R. G., Campante, T. L., Chaplin, W. J., Cunha, M. S., Lund, M. N., Kiefer, R., et al. (2018). Signatures of magnetic activity in the seismic data of solar-type stars observed by kepler. *ApJS* 237, 17. doi:10.3847/1538-4365/aac9b6

Santos, A. R. G., García, R. A., Mathur, S., Bugnet, L., Saders, J. L. v., Metcalfe, T. S., et al. (2019). Surface rotation and photometric activity for kepler targets. I. M and K Main-sequence stars. *ApJS* 244, 21. doi:10.3847/1538-4365/ab3b56

Santos, A. R. G., Mathur, S., García, R. A., Broomhall, A. M., Egeland, R., Jiménez, A., et al. (2023). Temporal variation of the photometric magnetic activity for the Sun and Kepler solar-like stars. *A&A* 672, A56. doi:10.1051/0004-6361/202245430

Saunders, N., van Saders, J. L., Lyttle, A. J., Metcalfe, T. S., Li, T., Davies, G. R., et al. (2023). Stellar cruise control: weakened magnetic braking leads to sustained rapid rotation of old stars. *ApJ* 962, 138. doi:10.3847/1538-4357/ad1516

Schmitt, J. H. M. M., Fleming, T. A., and Giampapa, M. S. (1995). The X-ray view of the low-mass stars in the solar neighborhood. *ApJ* 450, 392. doi:10.1086/176149

Schunker, H., Schou, J., and Ball, W. H. (2016a). Asteroseismic inversions for radial differential rotation of Sun-like stars: sensitivity to uncertainties. *A&A* 586, A24. doi:10.1051/0004-6361/201525937

Schunker, H., Schou, J., Ball, W. H., Nielsen, M. B., and Gizon, L. (2016b). Asteroseismic inversions for radial differential rotation of Sun-like stars: ensemble fits. *A&A* 586, A79. doi:10.1051/0004-6361/201527485

See, V., Matt, S. P., Finley, A. J., Folsom, C. P., Boro Saikia, S., Donati, J.-F., et al. (2019a). Do non-dipolar magnetic fields contribute to spin-down torques? *ApJ* 886, 120. doi:10.3847/1538-4357/ab46b2

See, V., Matt, S. P., Folsom, C. P., Boro Saikia, S., Donati, J.-F., Fares, R., et al. (2019b). Estimating magnetic filling factors from zeeman-Doppler magnetograms. *ApJ* 876, 118. doi:10.3847/1538-4357/ab1096

See, V., Roquette, J., Amard, L., and Matt, S. (2023). Further evidence of the link between activity and metallicity using the flaring properties of stars in the Kepler field. *MNRAS* 524, 5781–5786. doi:10.1093/mnras/stad2020

See, V., Roquette, J., Amard, L., and Matt, S. P. (2021). Photometric variability as a proxy for magnetic activity and its dependence on metallicity. *ApJ* 912, 127. doi:10.3847/1538-4357/abed47

Semel, M. (1989). Zeeman-Doppler imaging of active stars. I - basic principles. *A&A* 225, 456–466.

Shapiro, A. I., Solanki, S. K., Krivova, N. A., Yeo, K. L., and Schmutz, W. K. (2016). Are solar brightness variations faculae- or spot-dominated?. *A&A* 589, A46. doi:10.1051/0004-6361/201527527

Shoda, M., Cranmer, S. R., and Toriumi, S. (2023). Formulating mass-loss rates for sun-like stars: a hybrid model approach. *ApJ* 957, 71. doi:10.3847/1538-4357/acfa72

Shoda, M., Suzuki, T. K., Matt, S. P., Cranmer, S. R., Vidotto, A. A., Strugarek, A., et al. (2020). Alfvén-wave-driven magnetic rotator winds from low-mass stars. i. rotation dependences of magnetic braking and mass-loss rate. *ApJ* 896, 123. doi:10.3847/1538-4357/ab94bf

Silva-Beyer, J., Godoy-Rivera, D., and Chanamé, J. (2023). The breakdown of current gyrochronology as evidenced by old coeval stars. *MNRAS* 523, 5947–5961. doi:10.1093/mnras/stad1803

Simonian, G. V. A., Pinsonneault, M. H., and Terndrup, D. M. (2019). Rapid rotation in the kepler field: not a single star phenomenon. *ApJ* 871, 174. doi:10.3847/1538-4357/aaf97c

Skumanich, A. (1972). Time scales for CA II emission decay, rotational braking, and lithium depletion. *ApJ* 171, 565. doi:10.1086/151310

Soderblom, D. R., Duncan, D. K., and Johnson, D. R. H. (1991). The chromospheric emission–age relation for stars of the lower main sequence and its implications for the star formation rate. *ApJ* 375, 722. doi:10.1086/170238

Soderblom, D. R., Stauffer, J. R., Hudon, J. D., and Jones, B. F. (1993). Rotation and chromospheric emission among F, G, and K dwarfs of the Pleiades. *ApJS* 85, 315. doi:10.1086/191767

Solanki, S. K. (2003). Sunspots: an overview. *A&ARv* 11, 153–286. doi:10.1007/s00159-003-0018-4

Soon, W. H., Baliunas, S. L., and Zhang, Q. (1993). An interpretation of cycle periods of stellar chromospheric activity. *ApJ* 414, L33. doi:10.1086/186989

Spada, F., and Lanzafame, A. C. (2020). Competing effect of wind braking and interior coupling in the rotational evolution of solar-like stars. *A&A* 636, A76. doi:10.1051/0004-6361/201936384

Stauffer, J. R., and Hartmann, L. W. (1987). The distribution of rotational velocities for low-mass stars in the Pleiades. *ApJ* 318, 337. doi:10.1086/165371

Stauffer, J. R., Schultz, G., and Kirkpatrick, J. D. (1998). Keck spectra of Pleiades Brown dwarf candidates and a precise determination of the lithium depletion edge in the Pleiades. *ApJ* 499, L199–L203. doi:10.1086/311379

Strugarek, A. (2018). "Models of star-planet magnetic interaction," in *Handbook of exoplanets*. Editors H. J. Deeg, and J. A. Belmonte (Cham: Springer International Publishing), 1833–1855. doi:10.1007/978-3-319-55333-7_25

Suárez Mascareño, A., Rebolo, R., González Hernández, J. I., and Esposito, M. (2017). Characterization of the radial velocity signal induced by rotation in late-type dwarfs. *MNRAS* 468, 4772–4781. doi:10.1093/mnras/stx771

Thomas, A. E. L., Chaplin, W. J., Davies, G. R., Howe, R., Santos, A. R. G., Elsworth, Y., et al. (2019). Asteroseismic constraints on active latitudes of solar-type stars: HD 173701 has active bands at higher latitudes than the Sun. *MNRAS* 485, 3857–3868. doi:10.1093/mnras/stz672

Tokuno, T., Suzuki, T. K., and Shoda, M. (2023). Transition of latitudinal differential rotation as a possible cause of weakened magnetic braking of solar-type stars. *MNRAS* 520, 418–436. doi:10.1093/mnras/stad103

Torres, G., Vanderburg, A., Curtis, J. L., Kraus, A. L., Rizzuto, A. C., and Ireland, M. J. (2020). Eclipsing binaries in the open cluster Ruprecht 147. III. The triple system EPIC 219552514 at the main-sequence turnoff. *ApJ* 896, 162. doi:10.3847/1538-4357/ab911b

Tripathy, S. C., Jain, K., Salabert, D., García, R. A., Hill, F., and Leibacher, J. W. (2011). Angular-degree dependence of p-mode frequencies during solar cycle 23. *J. Phys. Conf. Ser.* 271, 012055. doi:10.1088/1742-6596/271/1/012055

Valenti, J. A., and Fischer, D. A. (2005). Spectroscopic properties of cool stars (SPOCS). I. 1040 F, G, and K dwarfs from keck, lick, and AAT planet search programs. *ApJS* 159, 141–166. doi:10.1086/430500

van Driel-Gesztelyi, L., and Green, L. M. (2015). Evolution of active regions. *Living Rev. Sol. Phys.* 12, 1. doi:10.1007/lrsp-2015-1

van Saders, J. L., Ceillier, T., Metcalfe, T. S., Silva Aguirre, V., Pinsonneault, M. H., García, R. A., et al. (2016). Weakened magnetic braking as the origin of anomalously rapid rotation in old field stars. *Nature* 529, 181–184. doi:10.1038/nature16168

van Saders, J. L., and Pinsonneault, M. H. (2012). The sensitivity of convection zone depth to stellar abundances: an absolute stellar abundance scale from asteroseismology. *ApJ* 746, 16. doi:10.1088/0004-637X/746/1/16

van Saders, J. L., and Pinsonneault, M. H. (2013). Fast star, slow star; old star, young star: subgiant rotation as a population and stellar physics diagnostic. *ApJ* 776, 67. doi:10.1088/0004-637X/776/2/67

van Saders, J. L., Pinsonneault, M. H., and Barbieri, M. (2019). Forward modeling of the kepler stellar rotation period distribution: interpreting periods from mixed and biased stellar populations. *ApJ* 872, 128. doi:10.3847/1538-4357/aafafe

Vaughan, A. H. (1980). Comparison of activity cycles in old and young main-sequence stars. *PASP* 92, 392–396. doi:10.1086/130684

Vaughan, A. H., and Preston, G. W. (1980). A survey of chromospheric CA II H and K emission in field stars of the solar neighborhood. *PASP* 92, 385–391. doi:10.1086/130683

Vidotto, A. A., Gregory, S. G., Jardine, M., Donati, J. F., Petit, P., Morin, J., et al. (2014). Stellar magnetism: empirical trends with age and rotation. *MNRAS* 441, 2361–2374. doi:10.1093/mnras/stu728

Walter, F. M., and Bowyer, S. (1981). On the coronae of rapidly rotating stars. I. The relation between rotation and coronal activity in RS CVn systems. *ApJ* 245, 671–676. doi:10.1086/158842

Weber, E. J., and Davis, L., Jr. (1967). The angular momentum of the solar wind. *ApJ* 148, 217–227. doi:10.1086/149138

Wilson, O. C. (1963). A probable correlation between chromospheric activity and age in main-sequence stars. *ApJ* 138, 832. doi:10.1086/147689

Wilson, O. C. (1968). Flux measurements at the centers of stellar H- and K-lines. *ApJ* 153, 221. doi:10.1086/149652

Wilson, O. C. (1978). Chromospheric variations in main-sequence stars. *ApJ* 226, 379–396. doi:10.1086/156618

Wood, B. E., Müller, H.-R., Redfield, S., Konow, F., Vannier, H., Linsky, J. L., et al. (2021). New observational constraints on the winds of M dwarf stars ∗ . *ApJ* 915, 37. doi:10.3847/1538-4357/abfda5

Woodard, M. F., and Noyes, R. W. (1985). Change of solar oscillation eigenfrequencies with the solar cycle. *Nature* 318, 449–450. doi:10.1038/318449a0

Wright, N. J., and Drake, J. J. (2016). Solar-type dynamo behaviour in fully convective stars without a tachocline. *Nature* 535, 526–528. doi:10.1038/nature18638

Wright, N. J., Drake, J. J., Mamajek, E. E., and Henry, G. W. (2011). The stellar-activity-rotation relationship and the evolution of stellar dynamos. *ApJ* 743, 48. doi:10.1088/0004-637X/743/1/48

Wright, N. J., Newton, E. R., Williams, P. K. G., Drake, J. J., and Yadav, R. K. (2018). The stellar rotation–activity relationship in fully convective M dwarfs. *MNRAS* 479, 2351–2360. doi:10.1093/mnras/sty1670

Yang, H., and Liu, J. (2019). The flare catalog and the flare activity in the kepler mission. *ApJS* 241, 29. doi:10.3847/1538-4365/ab0d28

Zhong, M., Zhang, L., Yang, Z., and Su, T. (2023). Magnetic activity of different types of variable stars observed by TESS mission. *Universe* 9, 227. doi:10.3390/universe9050227

Zirin, H. (1970). Active regions. I: the occurrence of solar flares and the development of active regions. *Sol. Phys.* 14, 328–341. doi:10.1007/BF00221318